

- This document has been reproduced from the best copy furnished by the organizational source. It is being released in the interest of making available as much information as possible.
- This document may contain data, which exceeds the sheet parameters. It was furnished in this condition by the organizational source and is the best copy available.
- This document may contain tone-on-tone or color graphs, charts and/or pictures, which have been reproduced in black and white.
- This document is paginated as submitted by the original source.
- Portions of this document are not fully legible due to the historical nature of some of the material. However, it is the best reproduction available from the original submission.

X-490-71-44

PREPRINT

NASA TM X-65507

**SUMMARY REPORT
ABSORPTION EFFECTS ON
VHF PROPAGATION BETWEEN
SYNCHRONOUS SATELLITES
AND AIRCRAFT**

E. J. MUELLER

DECEMBER 1970



— GODDARD SPACE FLIGHT CENTER —

GREENBELT, MARYLAND

N71-24914

(ACCESSION NUMBER)

50

(PAGES)

TMX-65507

(NASA CR OR TMX OR AD NUMBER)

(THRU)

63

(CODE)

07

(CATEGORY)



SUMMARY REPORT
ABSORPTION EFFECTS ON VHF PROPAGATION
BETWEEN SYNCHRONOUS SATELLITE AND AIRCRAFT

EDWARD J. MUELLER*

DECEMBER 1970

GODDARD SPACE FLIGHT CENTER
GREENBELT, MARYLAND

* WESTINGHOUSE ELECTRIC CORP., FIELD ENGINEERING AND SUPPORT
P.O. BOX 1693, BALTIMORE, MARYLAND 21203

SUMMARY REPORT
ABSORPTION EFFECTS ON VHF PROPAGATION
BETWEEN SYNCHRONOUS SATELLITE AND AIRCRAFT

EDWARD J. MUELLER*

DECEMBER 1970

GODDARD SPACE FLIGHT CENTER
GREENBELT, MARYLAND

* WESTINGHOUSE ELECTRIC CORP., FIELD ENGINEERING AND SUPPORT
P.O. BOX 1693, BALTIMORE, MARYLAND 21203

TABLE OF CONTENTS

| <u>Paragraph</u> | <u>Page</u> |
|--|-------------|
| 1.0 INTRODUCTION | 1 |
| 2.0 TROPOSPHERIC ABSORPTION. | 2 |
| 3.0 IONOSPHERIC ABSORPTION | 2 |
| 3.1 General. | 2 |
| 3.2 Auroral Absorption | 4 |
| 3.2.1 General. | 4 |
| 3.2.2 Latitudinal and Longitudinal Dependence. | 4 |
| 3.2.3 Diurnal Dependence | 6 |
| 3.2.4 Seasonal Dependence. | 6 |
| 3.2.5 Solar Dependence | 8 |
| 3.2.6 Frequency Dependence | 8 |
| 3.2.7 Elevation Angle Dependence | 9 |
| 3.2.8 Magnitude and Statistics | 9 |
| 3.2.9 Geographical Distribution in North Atlantic. | 11 |
| 3.2.10 Conclusions. | 21 |
| 3.3 Polar Cap Absorption | 21 |
| 3.3.1 General. | 21 |
| 3.3.2 Latitudinal and Longitudinal Dependence. | 22 |
| 3.3.3 Solar Dependence | 22 |
| 3.3.4 Diurnal Dependence | 23 |
| 3.3.5 Seasonal Dependence. | 23 |
| 3.3.6 Frequency Dependence | 23 |
| 3.3.7 Elevation Angle Dependence | 26 |
| 3.3.8 Magnitude and Statistics | 26 |
| 3.3.9 Geographical Distribution of PCA in the North Atlantic | 29 |
| 3.3.10 Conclusions. | 32 |
| 4.0 SUMMARY AND RECOMMENDATIONS. | 41 |
| REFERENCES | 44 |

LIST OF ILLUSTRATIONS

| <u>Figure No.</u> | | <u>Page</u> |
|-------------------|--|-------------|
| 1 | Approximate Boundaries of the Northern Auroral Absorption Zone | 5 |
| 2 | Diurnal Pattern of Auroral Absorption (Reproduced from Hartz, Montbriand, and Vogan, Ref. 12) | 7 |
| 3 | Elevation Angle Correction Factors for Ionospheric Absorption. | 10 |
| 4 | Auroral Absorption. | 12 |
| 5 | Contours of Auroral Absorption of 126-MHz Signals from a 60°W Equatorial Satellite (Best case geometric and frequency scaling) | 13 |
| 6 | Contours of Auroral Absorption of 136-MHz Signals from a 20°W Equatorial Satellite (Best case geometric and frequency scaling) | 15 |
| 7 | Contours of Auroral Absorption of 126-MHz Signals from a 60°W Equatorial Satellite (Worst case geometric and frequency scaling) | 17 |
| 8 | Contours of Auroral Absorption of 136-MHz Signals from a 20°W Equatorial Satellite (Worst case geometric and frequency scaling). | 19 |
| 9 | Diurnal Pattern of Polar Cap Absorption (Courtesy R. Cormier, AFCRL) | 24 |
| 10 | Pencil beam vertical incidence attenuation versus frequency deduced from multiple frequency riometer measurements at College, Alaska, during the sequence of solar proton events in July 1961. (Reproduced from Bennett & Rourke, Ref. 23.) | 25 |
| 11 | Polar Cap Absorption (Reproduced from Whitney, Ref. 24) | 30 |
| 12 | Contours of Polar Cap Absorption of 126-MHz Signals from a 60°W Equatorial Satellite (Best case geometric and frequency scaling) | 33 |
| 13 | Contours of Polar Cap Absorption of 126-MHz Signals from a 20°W Equatorial Satellite (Best case geometric and frequency scaling). | 35 |

LIST OF ILLUSTRATIONS (CONTINUED)

| | | |
|----|---|----|
| 14 | Contours of Polar Cap Absorption of 126-MHz Signals from a 60°W Equatorial Satellite(Worst case geometric and frequency scaling) | 37 |
| 15 | Contours of Polar Cap Absorption of 126-MHz Signals from a 20°W Equatorial Satellite(Worst case geometric and frequency scaling) | 39 |
| 16 | Contours of Oblique 137 MHz Absorption Relative to 30 MHz Polar Cap Absorption from a 40°W Equatorial Satellite. (Reproduced from Pope and Leinbach, Ref. 26) | 42 |

ACKNOWLEDGEMENT

This report has been prepared to summarize the present state of knowledge regarding ionospheric absorption characteristics at very high frequencies (VHF). It has been used to assist the U. S. panel member in the technical preparation for the ASTRA IV Panel Meeting in Montreal, January 1971. A number of corrections, suggestions and changes have been made as a result of review of the material by the U. S. technical preparation group. The U. S. members of this group are:

Mr. C. A. Petry
Aeronautical Radio Inc.

Mr. F. Clese
Aeronautical Radio Inc.

Mr. Roy Anderson
General Electric Co.

Mr. J. L. Lipscomb
DOT/Federal Aviation Administration

Mr. Charles A. Brooks
DOT/Federal Aviation Administration

Mr. Carlton Keys
DOT/Federal Aviation Administration

Mr. Harold Stein
DOT/Transportation Systems Center

Mr. Peter Engles
DOT/Transportation Systems Center

Mr. Daniel Brandel
DOT/Transportation Systems Center

Mr. Leo Keane
DOT/Transportation Systems Center

Mr. Larry McCabe
DOT/Transportation Systems Center

Mr. Herbert E. Whitney
Air Force Cambridge Research Lab.

Dr. Jules Aarons
Air Force Cambridge Research Lab.

Mr. James L. Baker
NASA/Goddard Space Flight Center

Mr. Tom Golden
NASA/Goddard Space Flight Center

Mr. Ed. Martin
COMSAT Corporation

Mr. Tom Calvit
COMSAT Corporation

Mr. Joe Pope
NOAA/Environmental Research
Laboratories

While these persons are not directly responsible for the contents herein their comments and criticisms are sincerely appreciated.

1.0 INTRODUCTION

Over the past several years, much effort has been expended in an attempt to size the power requirements for an aeronautical satellite system which would operate in the VHF band. One reason for this effort is the uncertainties surrounding the variability of the signal levels due to the propagation path. In particular the allowances that should be made for absorption, scintillation and multipath fading have not been ascertained with a high degree of confidence or agreement. Additionally, the degree to which these same propagation phenomena might affect ranging and position fixing accuracy has not been established.

This report has been prepared to summarize the current state of knowledge regarding tropospheric and ionospheric absorption at the VHF frequencies of interest for an aeronautical satellite system. Only the effect of these absorption factors on signal levels is considered, and this is done without involvement in aeronautical operational procedures or specific aeronautical telecommunications systems designs.

The magnitude of absorption that would be experienced by an aircraft in high latitude regions is geometrically dependent on the aircraft position in the polar region and the angle of penetration of the ionosphere in addition to many non-geometric factors. Therefore, this report attempts to summarize the absorption phenomena in terms of geographical contours. The North Atlantic region employing two geostationary satellite positions was chosen as an illustrative example. The geometric scaling employed could be expanded to cover other regions of the world and other satellite positions with appropriate assumptions for the longitudinal and latitudinal behavior of the absorption phenomena.

2.0 TROPOSPHERIC ABSORPTION

The atmospheric gases that are capable of absorbing electromagnetic energy are oxygen and water vapor. The attenuation caused by these absorbing gases is quite frequency dependent with abnormally large absorptions occurring at 22 GHz for water vapor and 60 GHz for oxygen. Since the total path attenuation is proportional to the length of the path, there is also a strong elevation angle dependence.⁽¹⁾

In the VHF frequency range of interest in this paper, the oxygen absorption predominates but is below .001 db per km. In the worst case of an aircraft on the ground with the path to a geostationary satellite viewed at a zero elevation angle, the total path absorption at 136 MHz would be less than 0.2 db. Accordingly, tropospheric absorption may be neglected in satellite to aircraft links.

3.0 IONOSPHERIC ABSORPTION

3.1 GENERAL

Unlike tropospheric absorption, ionospheric absorption may, at times, (when the ionosphere is disturbed*) produce a significant amount of attenuation at VHF frequencies. This absorption arises from transferral of energy to the medium when electrons in the ionosphere, set into vibration by the incident electromagnetic wave, collide with heavy particles.⁽²⁾

There are several types of ionospheric absorption events that have been identified and studied intensively by geophysicists over the years. Four major categories are: auroral absorption (A.A.), polar cap absorption (PCA), sudden ionospheric disturbances (SID)** and sudden commencement absorption (SCA).

* Absorption at VHF frequencies in the normal ionosphere is negligible.

** Sometimes called sudden cosmic noise absorption (SCNA).

The following table briefly identifies their basic characteristics. ⁽³⁾

| <u>Type</u> | <u>Association</u> | <u>Onset</u> | <u>Fade Duration</u> | <u>Geog. Distribution</u> |
|-------------|--------------------|--------------|----------------------|---------------------------|
| AA | Magnetic Activity | Concurrent | Min-Hours | Auroral Zone |
| PCA | Solar Flares | Delayed | Days | Both Polar Caps |
| SID | Solar Flares | Concurrent | Min-Hours | Sunlit Hemisphere |
| SCA | Magnetic Storms | Concurrent | Brief (Min) | Auroral Zone |

Only auroral and polar cap absorption are considered significant at VHF ⁽⁴⁾ and will be discussed in this paper.

Ionospheric absorption events are associated with precipitation of energetic particles into the ionosphere and their interaction with the earth's magnetic field. For purpose of studying ionospheric phenomena, geophysicists have employed various types of models for the earth's magnetosphere. The simplest model is the "dipole field" which is a first approximation based on a uniformly magnetized sphere in the direction of the centered dipole axis. ⁽⁵⁾ Much of the earlier data on ionospheric absorption was analyzed employing a coordinate system developed from this model. However, the real magnetic field is distorted from this "ideal" field due to solar influences and is not constant with time. In 1961, McIlwain ⁽⁶⁾ proposed a coordinate system based on "B, L space" where B is the magnitude of the total magnetic field (at any point) and L is a parameter calculated through the use of relationships among the adiabatic invariants that are valid in a static dipole field. The term "Invariant Geomagnetic Coordinates" has been applied to this system and it has gained wide acceptance as a standard system for comparison and systematization of ionospheric data. The maps showing invariant latitude used in this paper were prepared from tables contained in reference (7). An altitude of 300 Km was chosen to roughly coincide with the

F layer for scintillation studies. Therefore, there is a minor discrepancy (of less than one half degree) where this map is used for D region absorption studies in the high latitudes in this paper.

Although VHF signals from synchronous satellites have been monitored frequently by high latitude stations, there is no statistically significant data available which separates auroral and polar cap absorption from scintillation fading. In order to evaluate the effect of these types absorption, it is necessary to resort to scaling measurements taken at lower frequencies with techniques that do not geometrically correspond to the synchronous satellite to aircraft case. The literature is replete with data taken with 30 MHz vertical incidence riometers, monitoring of polar and auroral communications circuits at HF and VHF, and ionosonde recordings in the HF band. By far, the riometer data is more plentiful and perhaps easier to scale; therefore, it has been used as a data source in this report for the purpose of studying both auroral and polar absorption.

3.2 AURORAL ABSORPTION

3.2.1 General

Auroral absorption is produced by electrons with energies of only a few Kev which precipitate into the "D" region of the ionosphere between about 30 and 90 Km above the earth. ⁽⁸⁾⁽⁹⁾ It generally occurs during periods of magnetic activity and is associated with the incidence of visual aurora. ⁽⁸⁾

3.2.2 Latitudinal and Longitudinal Dependence

The northern auroral absorption zone is shown in Figure 1. The boundaries and band of maximum frequency of occurrence are estimated from vertical incidence riometer measurements in Canada ⁽¹²⁾ and Norway ⁽¹³⁾. Theoretically, the diurnal pattern seen by a station should depend somewhat on longitude;

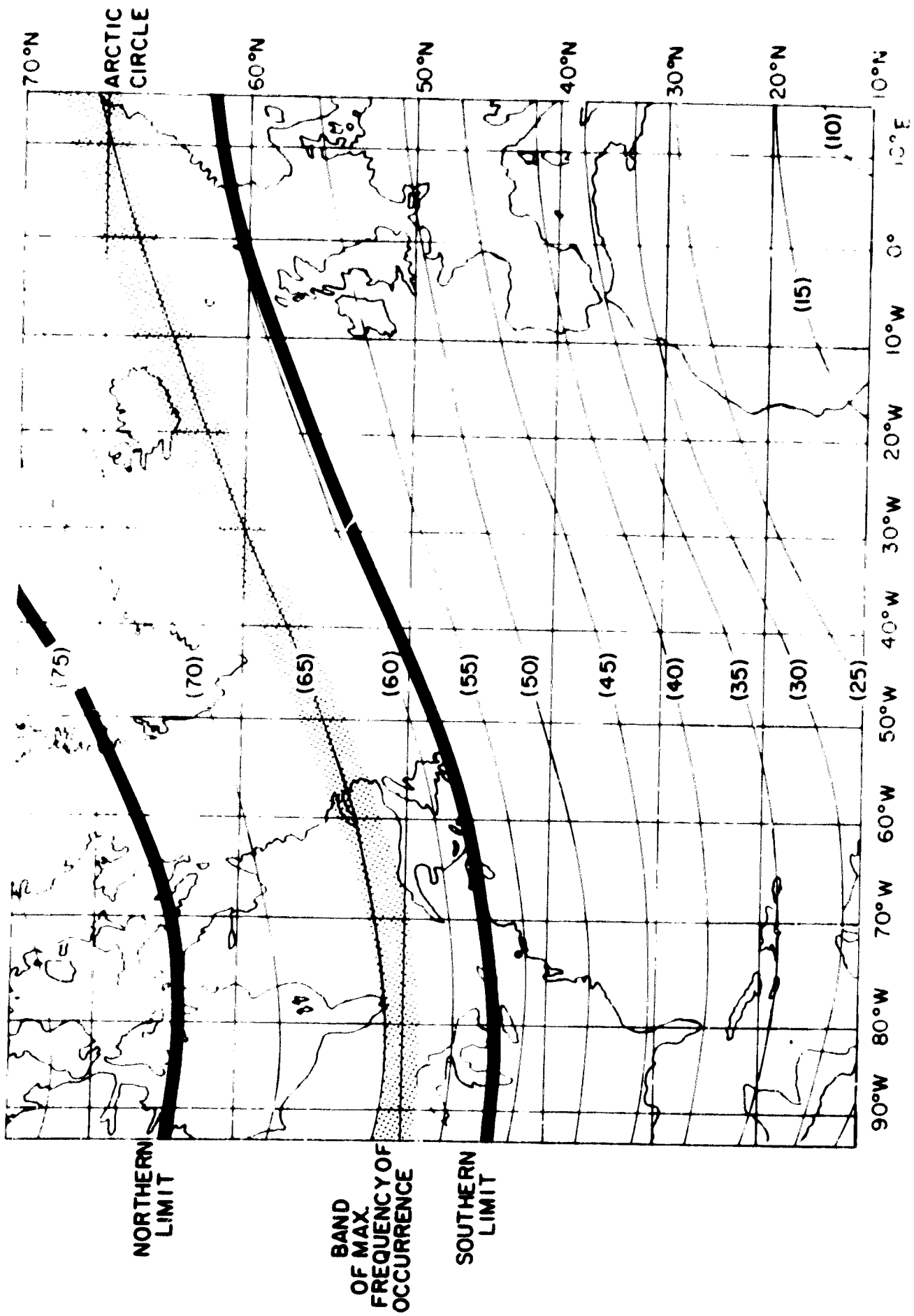


Figure 1. Approximate Boundaries of the Northern Auroral Absorption Zone (Estimated from Hartz, et al, Reference 12)

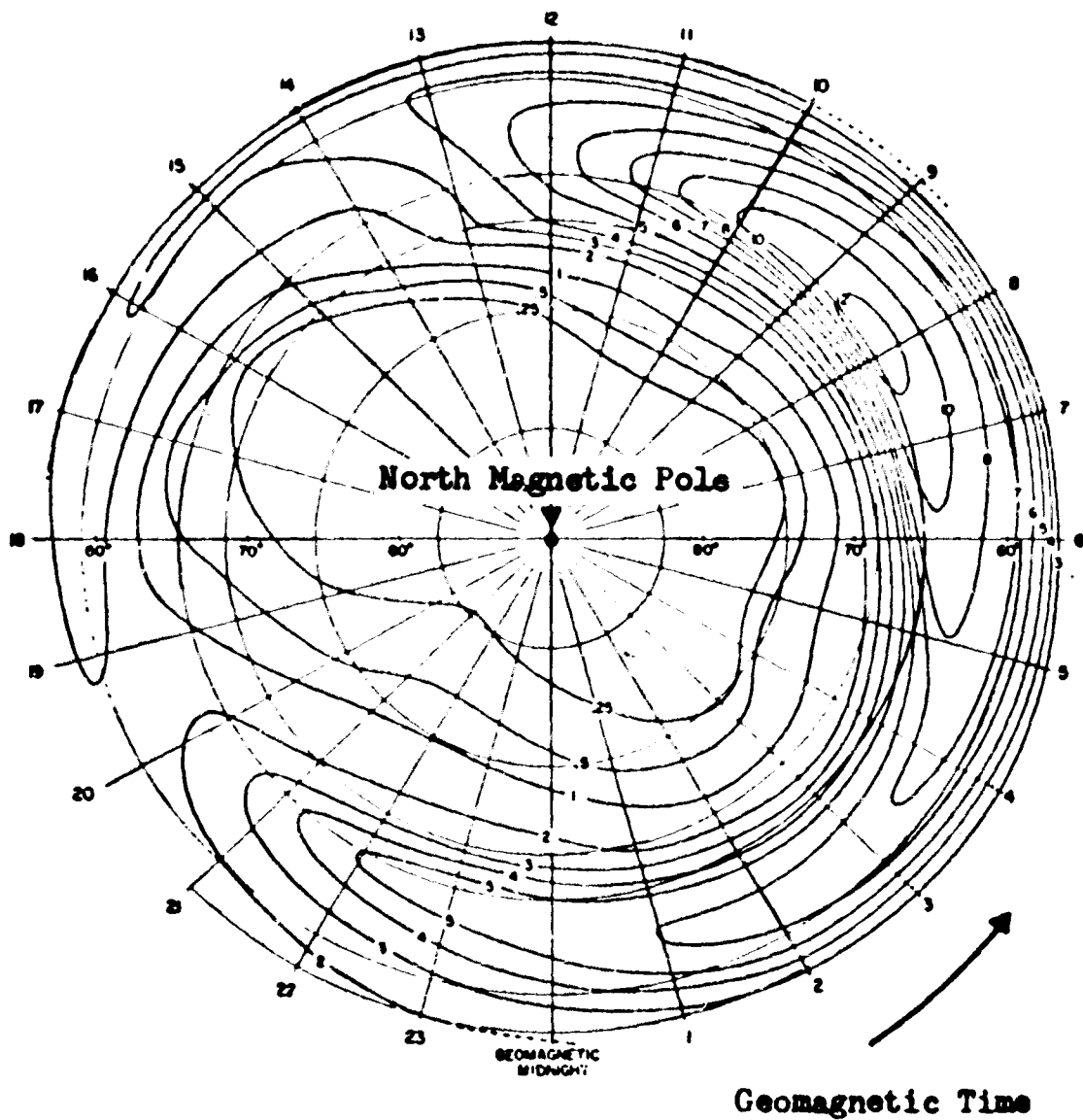
however, statistical analysis of available data has not been convincing of this effect⁽²⁾.

3.2.3 Diurnal Dependence

Auroral absorption displays a definite diurnal pattern with two pronounced maxima, one just before local midnight and the other some ten hours later⁽¹²⁾. Hargreaves⁽²⁾ describes a typical day to begin at about 2000 (field line time) with . . . "a spiky pattern, the absorption growing and decaying within a few minutes. Thereafter the variations become progressively smoother until, towards the end of the auroral day, the dominant variations take tens of minutes to an hour to two". The statistics of the diurnal pattern are best exemplified by Figure 2 which indicates the time percentage occurrence of 1.0 db or more absorption as a function of geomagnetic latitude and geomagnetic time.⁽¹²⁾ This data was obtained during a period of declining sunspot numbers from 1959-1961. It may be noted that about 0800 geomagnetic time 1 db or more absorption is exceeded 12% of the time at about 64.5° GML.

3.2.4 Seasonal Dependence

A pronounced annual change from winter maximum to summer minimum is evident in the Alaskan data⁽¹¹⁾. This seasonal variation, some 1 1/2 to 2 times greater in winter, is probably related to changes in the magnetosphere as the dipole axis tilts with respect to the solar wind⁽²⁾. There is also a small seasonal range in the position of the absorption zone amounting to 1 or 2 degrees of latitude wherein the zone tends to remain parallel to the ecliptic. In contrast to these findings in Alaska, there is no very consistent annual pattern found in the Canadian data⁽¹²⁾.



Notes:

- (1) Circles are geomagnetic latitude
- (2) Values on contours indicate time percentage occurrence of auroral absorption of 1.0 db or more.
- (3) Values are for 30 MHz vertical riometer data.

**Figure 2. Diurnal Pattern of Auroral Absorption
(Reproduced from Hartz, Montbriand, and Vogan, Ref. 12)**

3.2.5 Solar Dependence

Auroral absorption does not appear to be related directly to the more obvious measures of solar activity such as sunspot numbers, flare indices or 2800 MHz radio bursts⁽²⁾. Over the 11 year sunspot number cycle, absorption changes of 2:1 have been observed in the Alaska sector; however, the sunspot numbers fell by a ratio of 10:1. Basler and Owren⁽⁸⁾ report a well defined 27-day recurrence pattern (associated with the rotation period of the sun); however, Basler later reports an anticorrelation between absorption and the solar indices over the 27-day cycle.⁽¹⁵⁾

3.2.6 Frequency Dependence

The total absorption along a path may be determined by applying the classical Appleton-Hartree treatment. Numerically, the absorption A over a path dl is given by Hargreaves:⁽²⁾

$$A(\text{db}) = 4.6 \times 10^{-5} \int \frac{N \nu \, dl}{\nu^2 + (\omega \pm \omega_L)^2}$$

where

N = electron density in m^{-3}

ω = 2π x observation frequency in cycles per second.

ω_L = 2π x longitudinal component of the gyromagnetic frequency in Hz.

ν = electron collision frequency per second.

At VHF frequencies where $\omega \gg \omega_L$ and at higher altitudes where $\omega \gg \nu$, equation (1) will show a definite $1/f^2$ frequency dependence.

⁽⁹⁾ Riometer measurements have generally supported this dependency.

Lerfald, et al using an $(f \pm f_L)^{-n}$ dependency report a mean n of approximately 1.8 for riometer frequencies between 5 and 50 MHz at College, Alaska.

⁽¹⁰⁾ Belikovich, et al report n values between 1.88 and 1.98 for riometer frequencies of 25 and 40 MHz at Loparskaya (near Murmansk)

3.2.7 Elevation Angle Dependence

One of the more significant dependencies to be considered in a satellite to aircraft path is the elevation angle at which the aircraft views the satellite. Considering that auroral absorption occurs at the higher latitudes, an equatorial synchronous satellite will nearly always be viewed at relatively low elevation angles where the longer absorption path will cause significantly greater attenuation than that observed by the vertical riometers. A first approximation of total path absorption may be obtained by multiplying the vertical incidence absorption value in db by the secant of the zenith angle.⁽⁴⁾ Such an approximation is quite good at elevation angles of 40° or more but begins to exaggerate the loss at the more significant lower elevation angles since the ionospheric absorption layer is a shell rather than a flat sheet. Figure 3 shows the correction factor to be applied to the vertical incidence absorption by taking the actual D-layer geometry into consideration and compares it to the secant of the zenith angle.

3.2.8 Magnitude and Statistics

There is no data available on auroral absorption directly measured on a synchronous satellite path. Consequently, it is necessary that the available 27.6 MHz vertical riometer data be used to evaluate its effect on an aeronautical satellite system. To accomplish this, the statistical distribution of the riometer data must be determined and then scaled in frequency and elevation angle.

Basler⁽¹¹⁾ presents a statistical plot of 2213 points scaled at 15 minute intervals for data taken at College Alaska (in the maximum zone during an extremely disturbed month, (February 1958)). This data was further

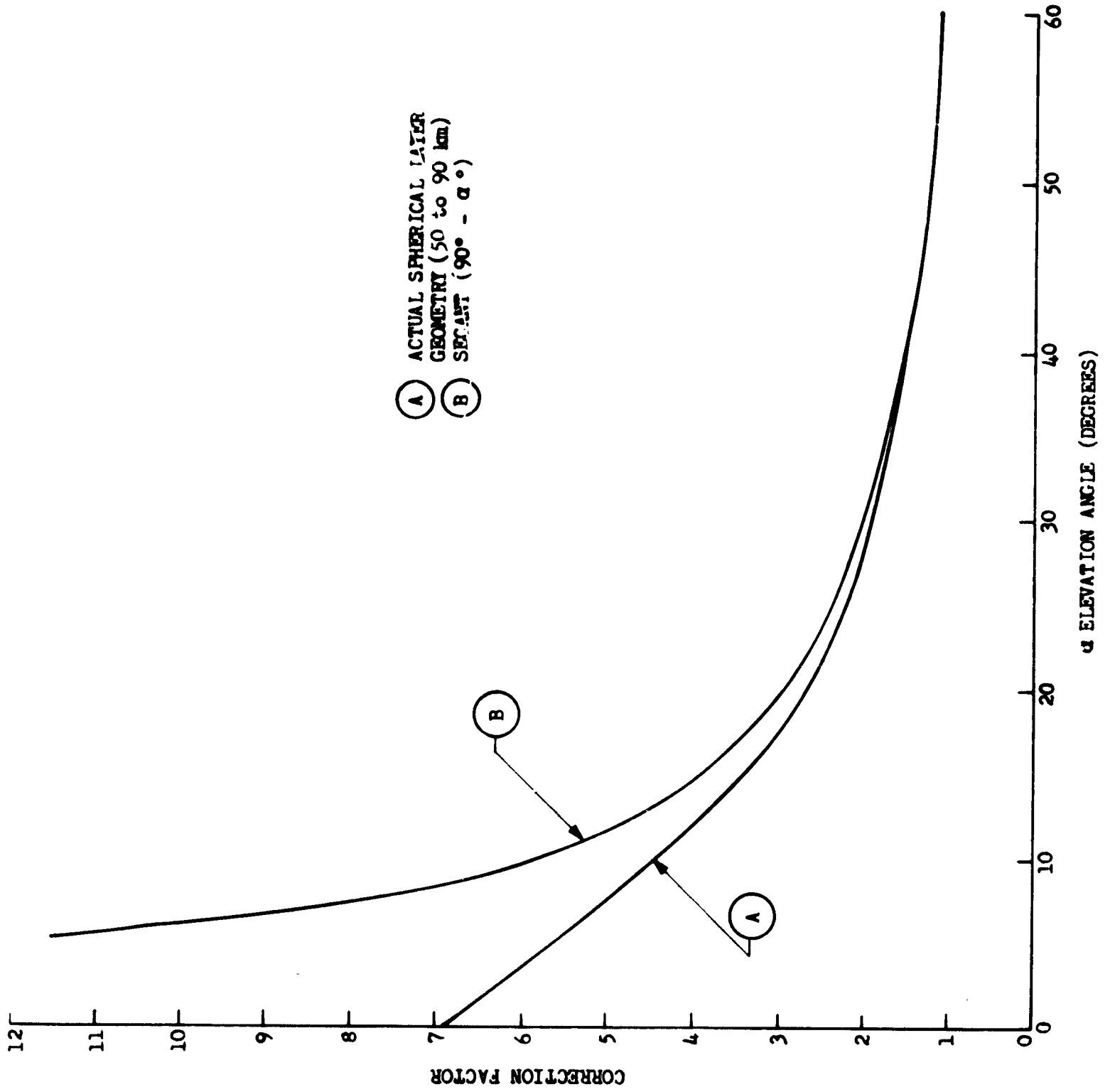


Figure 3. Elevation Angle Correction Factors for Ionospheric Absorption

scaled to 136 MHz at 10°, 20° and 30° elevation angles, and is shown in Figure 4 as scaled by Calvit⁽²⁵⁾. Figure 4 also shows data from Kiruna, Sweden similarly scaled⁽¹⁷⁾ (25). These statistical plots fairly well establish the order of magnitude of auroral absorption that might be expected by an aircraft flying in the auroral zone in communication through an equatorial geostationary satellite. For purposes of plotting the geographical contours, in this report, the curves for Kiruna were employed since they are based on some 6000 hours of data as compared to about 500 hours for the College data.

3.2 9 Geographical distribution in North Atlantic

The potential effect of auroral absorption on satellite to aircraft links can best be illustrated by examining the geographical distribution in a typical North Atlantic system model. The model employed in this paper consists of two geostationary satellites positioned at 20°W and 60°W. The data source employed is that extrapolated by Calvit⁽²⁵⁾ for Kiruna vertical riometer data⁽¹⁷⁾ which is assumed to apply along the maximum auroral absorption zone shown in Figure 1. Figures 5 through 8 depict contours of auroral absorption based on a number of assumptions which are defined in each map. Figures 5 and 7 apply to a 60°W satellite while Figures 6 and 8 apply to a 20°W satellite. The difference between assuming a combination of "best-case" frequency and elevation angle scaling, (i.e., scaling which favors less absorption) and that assuming "worst-case" scaling may be seen by comparing Figure 5 with Figure 7 and Figure 6 with Figure 8. Using the best case scaling assumptions ($1/f^2$ frequency and spherical D-layer elevation angle) it can be seen that auroral absorption should be less than 0.5 db for 99% of the time throughout the North Atlantic air traffic routes.

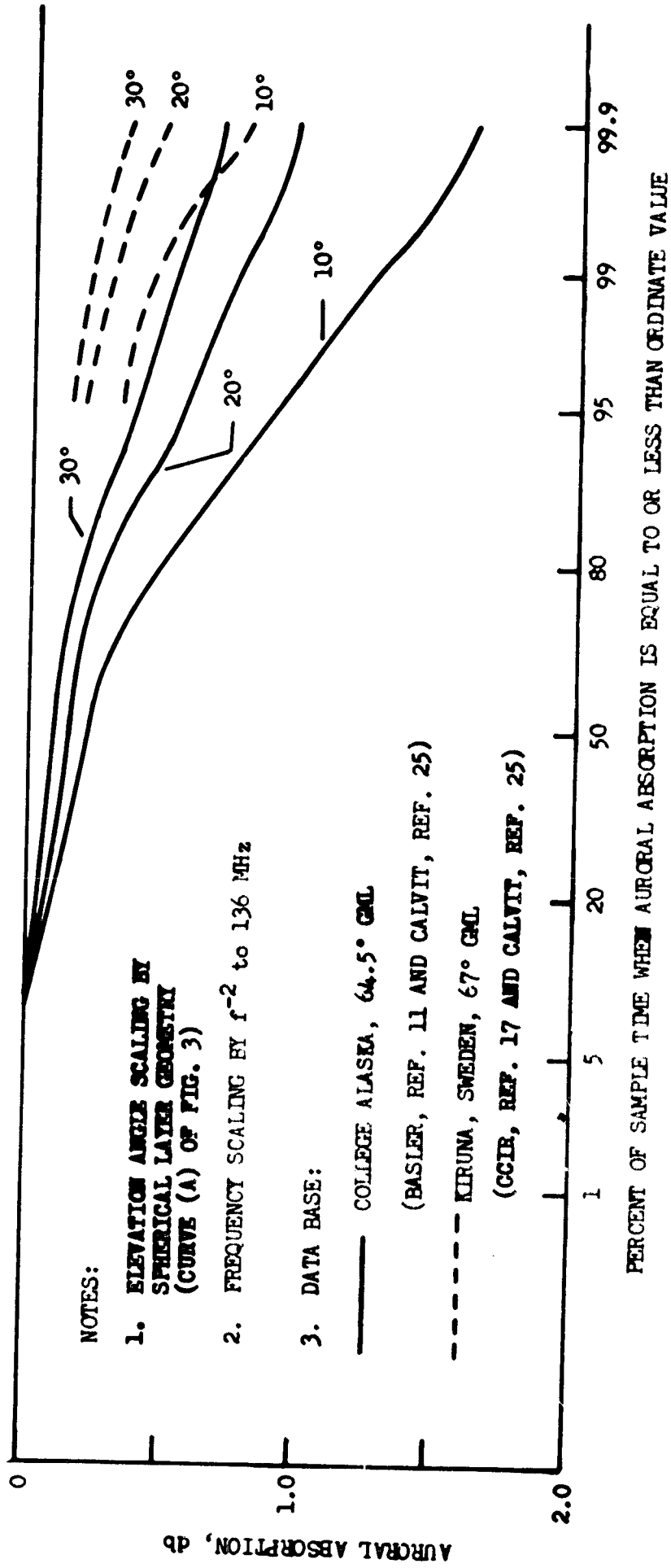


Figure 4. Auroral Absorption (After Calvit, Ref. 25)

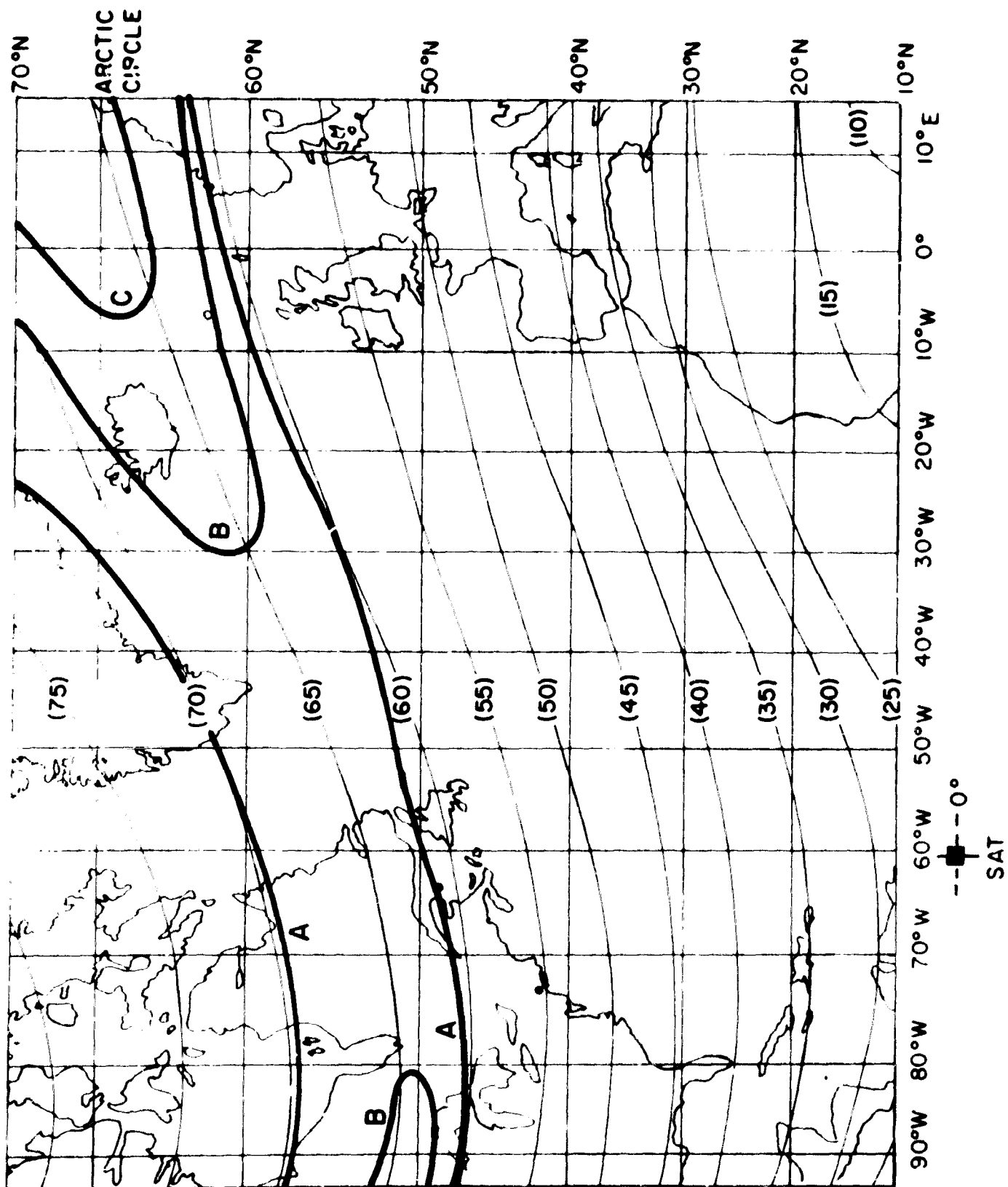


Figure 5. Contours of Auroral Absorption of 136 MHz Signals
 From a 60°W Equatorial Satellite (Best Case
 Geometric and Frequency Scaling)
 (See notes next page)

Figure 5. Contours of Auroral Absorption of 136 MHz Signals from a 60° W. Equatorial Satellite (Best case geometric and frequency scaling)

Notes: 1. Frequency scaling : $1/f^2$

2. Zenith angle scaling : Spherical D-layer (50 to 90 Km)

3. Absorption Contour values in db :

| <u>Contour</u> | <u>95%</u> | <u>99%</u> | <u>99.9%</u> |
|----------------|------------|------------|--------------|
| A | 0.1 | 0.2 | 0.25 |
| B | 0.2 | 0.3 | 0.5 |
| C | 0.4 | 0.6 | 1.0 |

4. Data Source: CCIR Document IV/1067, Ref.(17)

- a) Vertical riometer data at 27.6 MHz
- b) Kiruna, Sweden
- c) Date data was taken is not available.

5. Geographic extension assumptions:

- a) Absorption from data source applies along the maximum band shown in Fig. 1.
- b) Value drops to one half linearly with invariant latitude.
- c) One half values in vicinity of southern limit of auroral zone (see Fig. 1) and along the 70° invariant latitude line
- d) Absorption virtually zero at 55° invariant latitude.

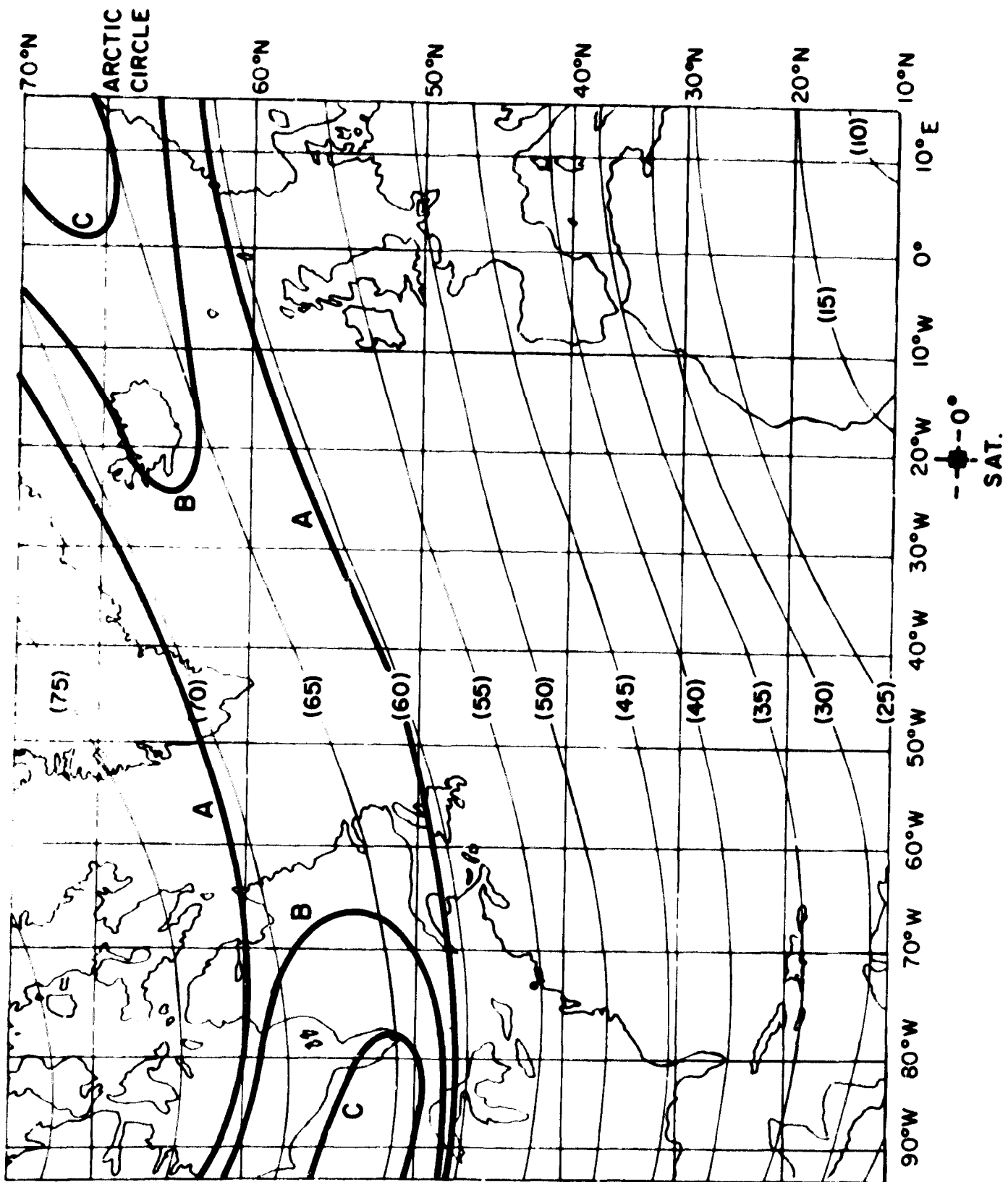


Figure 6. Contours of Auroral Absorption of 126 MHz Signals
 From a 20°W Equatorial Satellite (Best Case
 Geometric and Frequency Scaling)
 (See notes next page)

Figure 6. Contours of Auroral Absorption of 136 MHz Signals from a 20° W. Equatorial Satellite (Best case geometric and frequency scaling)

- Notes: 1. Frequency scaling: $1/f^2$
2. Zenith angle scaling: Spherical D-layer (50 - 90 km)

3. Absorption Contour values in db:

| <u>Contour</u> | <u>95%</u> | <u>99%</u> | <u>99.9%</u> |
|----------------|------------|------------|--------------|
| A | 0.1 | 0.2 | 0.25 |
| B | 0.2 | 0.3 | 0.5 |
| C | 0.4 | 0.6 | 1.0 |

4. Data Source: CCIR Document IX/1067, Ref. (17)

- a) Vertical Ricometer data at 27.6 MHz
 - b) Kiruna, Sweden
 - c) Data data was taken is not available
5. Geographic extension assumptions:

- a) Absorption from data source applies along the maximum band shown in Fig. 1.
- b) Value drops to one half linearly with invariant latitude.
- c) One half values in vicinity of southern limit of auroral zone (see Fig. 1) and along the 70° invariant line.
- d) Absorption virtually zero at 55° invariant latitude.

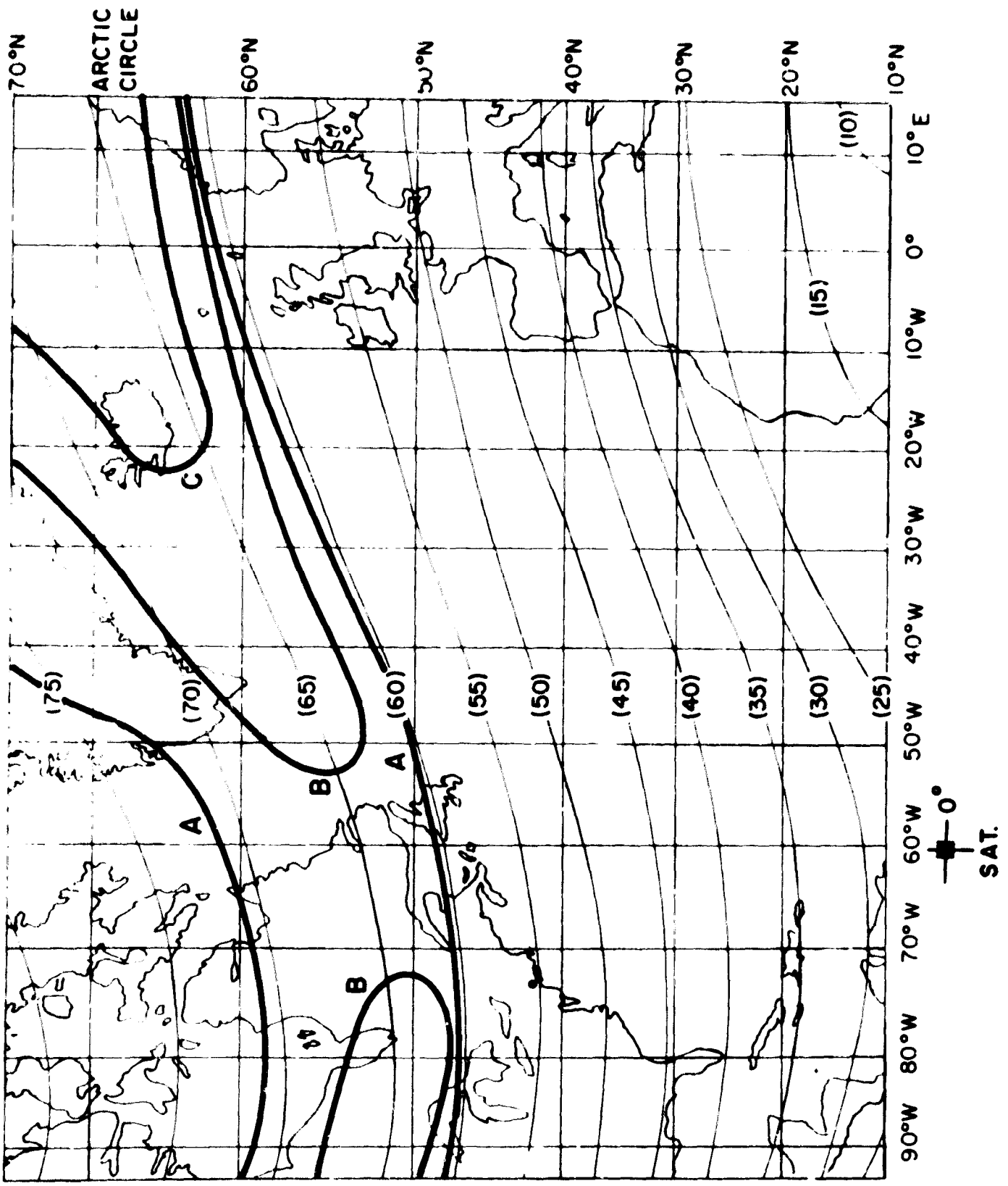


Figure 7. Contours of Auroral Absorption of 136MHz Signals
 From a 60°W Equatorial Satellite (Worst Case
 Geometric and Frequency Scaling)
 (See notes next page)

Figure 7. Contours of Auroral Absorption of 136 MHz
 Signals from a 60° W. Equatorial Satellite
 (Worst Case geometric and frequency scaling)

Notes: 1. Frequency scaling: $1/f^{1.8}$

2. Zenith angle scaling: Secant

3. Absorption Contour values in db:

| <u>Contour</u> | <u>95%</u> | <u>99%</u> | <u>99.9%</u> |
|----------------|------------|------------|--------------|
| A | 0.1 | 0.2 | 0.25 |
| B | 0.2 | 0.3 | 0.5 |
| C | 0.4 | 0.6 | 1.0 |

4. Data Source: CCIR Document IV/1067, Ref.(17)

a) Vertical Riometer data at 27.6 MHz

b) Kiruna, Sweden

c) Date data was taken is not available

5. Geographic extension assumptions:

- a) Absorption from data source applies along the maximum band shown in Fig. 1.
- b) Value drops to one half linearly with invariant latitude.
- c) One half values in vicinity of southern limit of auroral zone (see Fig. 1) and along the 70° invariant latitude line.
- d) Absorption virtually zero at 55° invariant latitude.

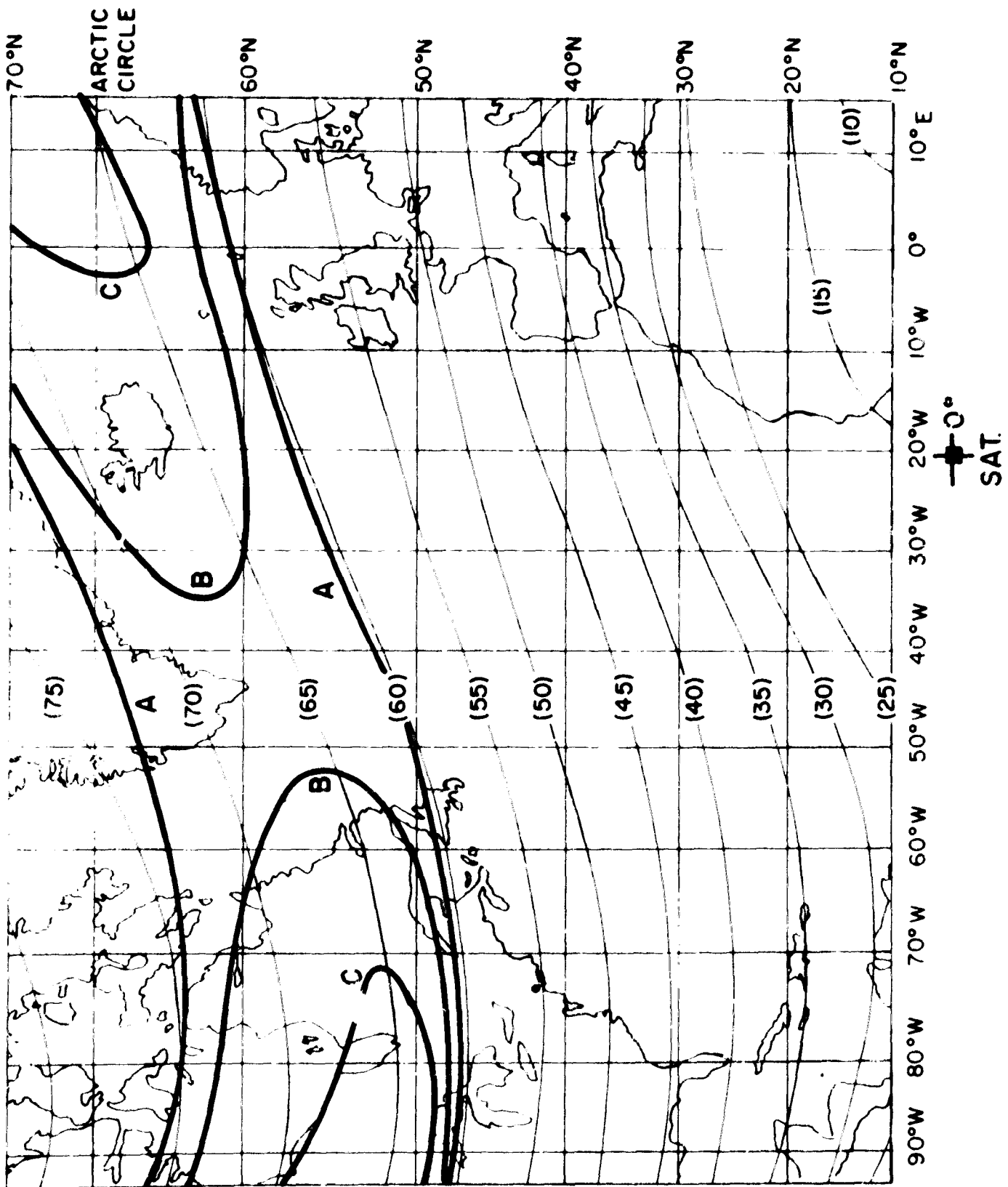


Figure 8. Contours of Auroral Absorption of 1260MHz Signals
 From a 20°W Equatorial Satellite (Worst Case
 Geometric and Frequency Scaling)
 (See notes next page)

Figure 8 . Contours of Auroral Absorption of 136 MHz
 Signals from a 20° W. Equatorial Satellite
 (Worst case geometric and frequency scaling)

Notes: 1. Frequency scaling: $1/f^{1.8}$

2. Zenith angle scaling: Secant

3. Absorption Contour values in db:

| <u>Contour</u> | <u>95%</u> | <u>99%</u> | <u>99.9%</u> |
|----------------|------------|------------|--------------|
| A | 0.1 | 0.2 | 0.25 |
| B | 0.2 | 0.3 | 0.5 |
| C | 0.4 | 0.6 | 1.0 |

4. Data Source: CCIR Document IV/1067, Ref. (17)

- a) Vertical Riometer data at 27.6 MHz
- b) Kiruna, Sweden
- c) Data data was taken is not available.

5. Geographic extension assumptions:

- a) Absorption from data source applies along the maximum band shown in Fig. 1.
- b) Value drops to one half linearly with invariant latitude.
- c) One half values in vicinity of southern limit of auroral zone (see Fig. 1) and along the 70° invariant latitude line.
- d) Absorption virtually zero at 55° invariant latitude.

Using the worst case assumptions some of the more northern regions of the ocean might experience absorption up to 0.7 db for 1% of the time.

3.2.10 Conclusions

In evaluating auroral absorption independently of other statistical propagation variables such as scintillation and multipath, it appears reasonable to conclude that no allowance need be made in a system power budget for a system requiring only 95% propagation time availability. However, systems requiring 99% or greater time availability should take such absorption into consideration, since between 1 - 2 db may be encountered in some geographical areas. However, since auroral absorption events generally last in the order of tens of minutes to an hour or two, are not correlated with multipath, and have been shown to be partially correlated with scintillation,⁽²⁷⁾ allowance should not be made by adding the magnitude db-wise into a power budget. Rather, the absorption statistics should be combined with the statistics of other types of fading employing a time frame suited to the aeronautical operations and modulation techniques employed in the system. In this manner, the added margin required to protect against auroral absorption events, even in the worst case, may have negligible impact on the system power budget.

3.3 POLAR CAP ABSORPTION

3.3.1 General

Polar cap absorption is produced by protons with energies up to a few hundred MeV which are expelled from the sun at the time of certain flares. PCA's may be a more serious threat to satellite to aircraft systems than auroral events since the attenuation of a radio wave may be considerably greater during some intense PCA events and they may also be of longer duration.

3.3.2 Latitudinal and Longitudinal Dependence

Polar cap absorption, as its name implies is normally confined to high geomagnetic latitudes and forms a more-or-less uniform blanket over the polar caps of the earth which may be defined in the northern hemisphere as the region north of about 64° geomagnetic latitude.⁽³⁾ However, it has been found that the edge of the PCA may move as far south as 55° - 58° GML several days after onset when a flare is followed by a sudden commencement magnetic storm.⁽¹⁸⁾⁽²¹⁾ The total duration of a PCA varies with latitude and may extend to 15 days in the most northerly regions.⁽¹⁸⁾⁽¹⁹⁾

3.3.3 Solar Dependence

Polar cap absorption usually sets in within a few hours of certain intense solar flares; however, the relationship between the particle producing properties and optical features of the flares is not yet established⁽³⁾. The sequence of absorption events accompanying PCA has been described by Reid and Leinbach as follows:⁽¹⁸⁾

- a) A major flare usually (but not always) of visual importance 3 or 3+ takes place on the sun. The flare often is accompanied by a SID over the sunlit hemisphere of the earth, and also by an intense solar radio noise storm of long duration.
- b) Within several hours after the flare, strong VHF radio wave absorption sets in over the polar cap. The absorption attains its maximum within a few more hours, and then begins to decay, taking from two or three days up to 15 days in the extreme case.
- c) Two or three days after the flare, a SCA (magnetic storm) usually occurs, often of great intensity. (The SCA may be accompanied by bright visual auroral displays and strong auroral absorption.

The frequency of PCA events varies in phase with the sunspot cycle and does not show a 27-day (solar rotation) recurrence tendency⁽⁸⁾. Bailey⁽¹⁹⁾ has catalogued the principal PCA events from 1952 to 1963 which showed none for the years 1952 through 1955 and 1962 (low sunspot numbers) and a significant number (some with equivalent 30 MHz riometer absorptions up to 23.7 db) in the high sunspot years of 1957-1959.

3.3.4 Diurnal Dependence

During the decay period, the absorption exhibits a pronounced diurnal variation as shown in Figure 9 for three locations during the PCA event of April 1969. Reid and Leinbach report that the daytime value is usually some four times greater (in decibels) than the nighttime values.⁽¹⁸⁾ However, a number of midday recoveries of up to half the total absorption,* lasting as long as 6-10 hours, have been reported.⁽²⁰⁾

3.3.5 Seasonal Dependence

There does not appear to be a correlation between PCA events and season of the year. However, the diurnal variation noted above is not observed at locations experiencing continuous daylight or darkness during an event indicating a relationship to solar illumination⁽³⁾.

3.3.6 Frequency Dependence

All the evidence to date seems to show that the inverse-square law is probably always fairly good for PCA events during nighttime conditions, but during daytime, the frequency exponent can vary quite widely according to the "hardness" of the proton spectrum, i.e., the relative numbers of high- and low-energy protons present.⁽²²⁾⁽²⁶⁾ This may be confirmed by noting the dependencies in Figure 10 which is reproduced from reference (23). It should be noted that on July 18 and 21, the 30 MHz/50 MHz dependency approached
* in db

PCA EVENT APRIL 1969

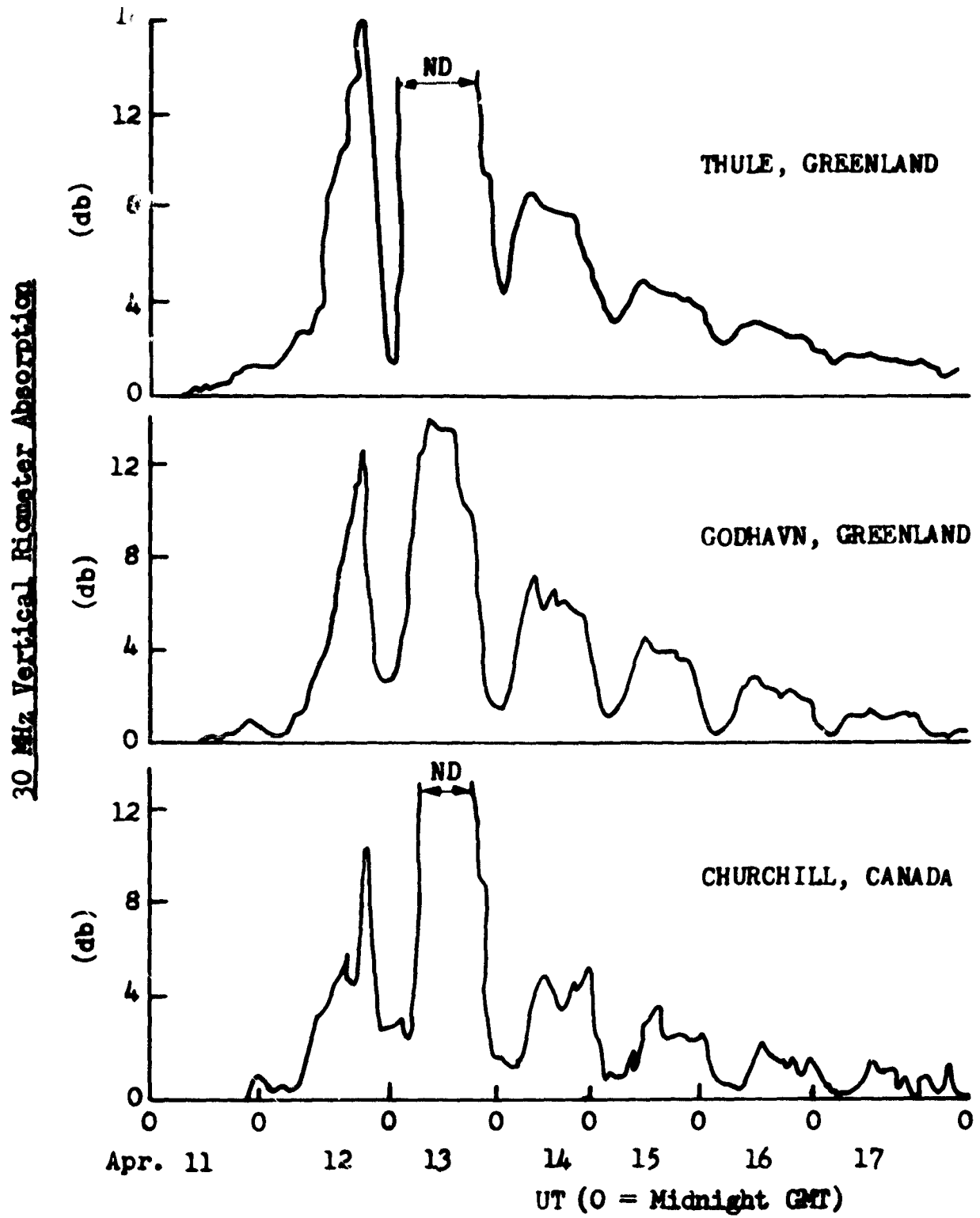


Figure 9. Diurnal Pattern of Polar Cap Absorption
(Courtesy R. Cormier, AFCRL)

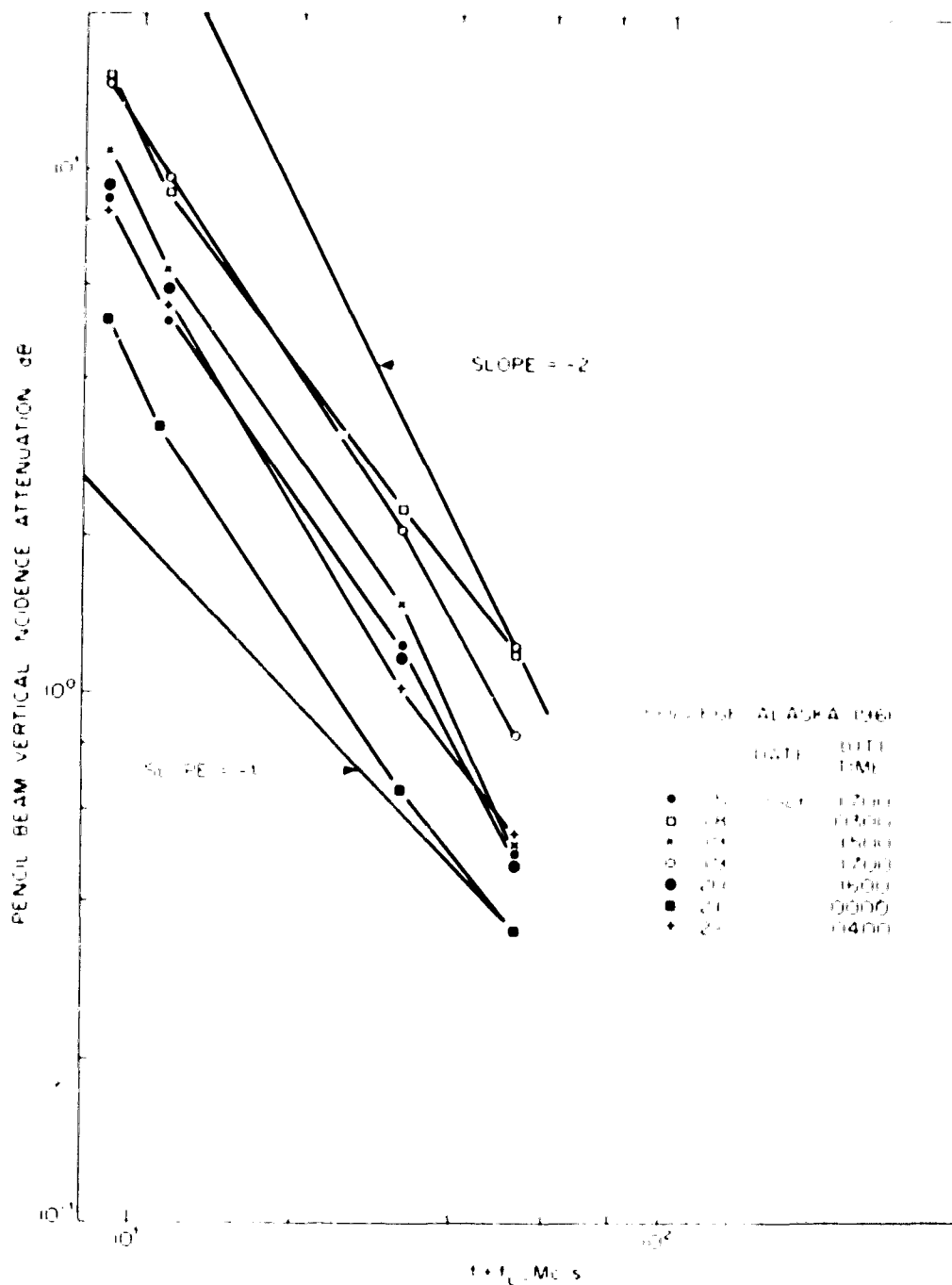


Figure 10. Pencil beam vertical incidence attenuation versus frequency deduced from multiple frequency riometer measurements at College, Alaska, during the sequence of solar proton events in July 1961.

(Reproduced from Bennett & Rourke, Ref. 23)

$1/f$ (during local daytime hours) and at the other times, this dependency approached $1/f^2$ (during local nighttime hours). Observations at Loparskaya (64° GML) during PCA events of July and September 1966 indicate a frequency dependence of $1/f^{1.5}$ and $1/f^{1.1}$ using test frequencies of 9 and 13 MHz.⁽¹⁰⁾ Although there is no direct measurements to support the extrapolation of these values to the vicinity of 136 MHz, Pope⁽²⁶⁾ theoretically supports values typically between 1.8 to slightly less than 1.5 depending on the cutoff energy and characteristic rigidity assumed for the ionosphere.

3.3.7 Elevation Angle Dependence

The elevation angle dependence of polar cap absorption is the same as that discussed under auroral absorption above.

3.3.8 Magnitude and Statistics

There is virtually no data available providing direct measurements of polar cap absorption on a path between a synchronous satellite and high latitude stations. Attempts to measure PCA at Thule on 136 MHz signals from ATS-3 during two events (29 October - 2 November 1968 and 11 April - 14 April 1969) were inconclusive.⁽²⁴⁾ Analysis of the satellite signal levels showed no evidence of decrease in average level corresponding to values expected from scaling of simultaneous 30MHz vertical riometer measurements. This scaling indicated 3 db or less PCA should have been observed on the satellite signals. During these attempts there was an accompanying magnetic storm which produced deep rapid fading. It was concluded that any absorption that occurred was small and could not be separated from the Faraday and scintillation fading.

The lack of direct measured data requires that the effect of PCA on an aeronautical satellite system be evaluated by extrapolating the 27.6 MHz riometer data that is available. In order to do this, three things must be considered: First, the peak values observed at the onset of an event and their

frequency of occurrence must be determined. Second, a model of the decay period and its statistical distribution must be established. And, third, the cumulative probability of the magnitude of absorption must be determined from the statistics of the peak values and diurnal model.

Peak Values of PCA

As previously discussed, Bailey⁽¹⁹⁾ has catalogued the peak value of all events exceeding 3 db (30 MHz vertical riometer equivalent) for the years 1952 through 1963. Further data covering the years 1956 through 1969 is tabulated by Whitney⁽²⁴⁾ and Pope⁽²⁶⁾. However, in the latter lists only events which would have produced 2 db or more PCA at 136 MHz and 10° elevation angle were included. The 30 MHz vertical riometer data was extrapolated by the inverse square of frequency and secant of the zenith angle. Inspection of this data leads one to conclude that the maximum peak 30 MHz value would be in order of 24 to 25 db. However, it is known that the vertical riometers and ionospheric scatter systems which were the sources of the basic data have limitations on the antenna beamwidth and dynamic range such that higher values might actually exist. This apparently led Basler et al⁽¹⁴⁾ to assume a maximum probable value of 30 db for the 27.6 MHz vertical (wide beam) riometer.

From the catalogues of Bailey and Whitney and Pope previously mentioned, the following table will give some indication of the frequency of occurrence of PCA's of various magnitudes. The table covers 1952 through 1969.

| PCA (db) | | No. of events equal to or exceeding value |
|------------------|--------------|--|
| 30 MHz. vertical | 136 MHz. 10° | |
| 7.2 | 2.0 | 26 |
| 11.2 | 3.0 | 17 |
| 14.5 | 4.0 | 9 |
| 22.0 | 6.0 | 3 |
| 23.7 | 6.5 | 2 |

Diurnal PCA Model

As pointed out earlier, a pronounced diurnal variation exists in

a PCA event and the envelope of the onset and decay period may vary from about three to ten days with an irregular structure including midday recoveries of up to half the total absorption. Thus, a PCA event does not lend itself readily to the development of a deterministic model. Perhaps a statistical model based on empirical data could be developed but it appears that this has not been done. One available model was originated by Levatic⁽¹⁶⁾ and published by the CCIR⁽¹⁷⁾. This model is arbitrary and assumes three twelve hour daytime periods with the peak value dropping each day to one-half the previous days value and the nighttime value dropping to about 1/15 the peak value of the first day. Pope⁽²⁶⁾ provides a five day model of the decay period but this was not used because it was based only on the high sunspot years of 1957-1960.

Cumulative probability of PCA

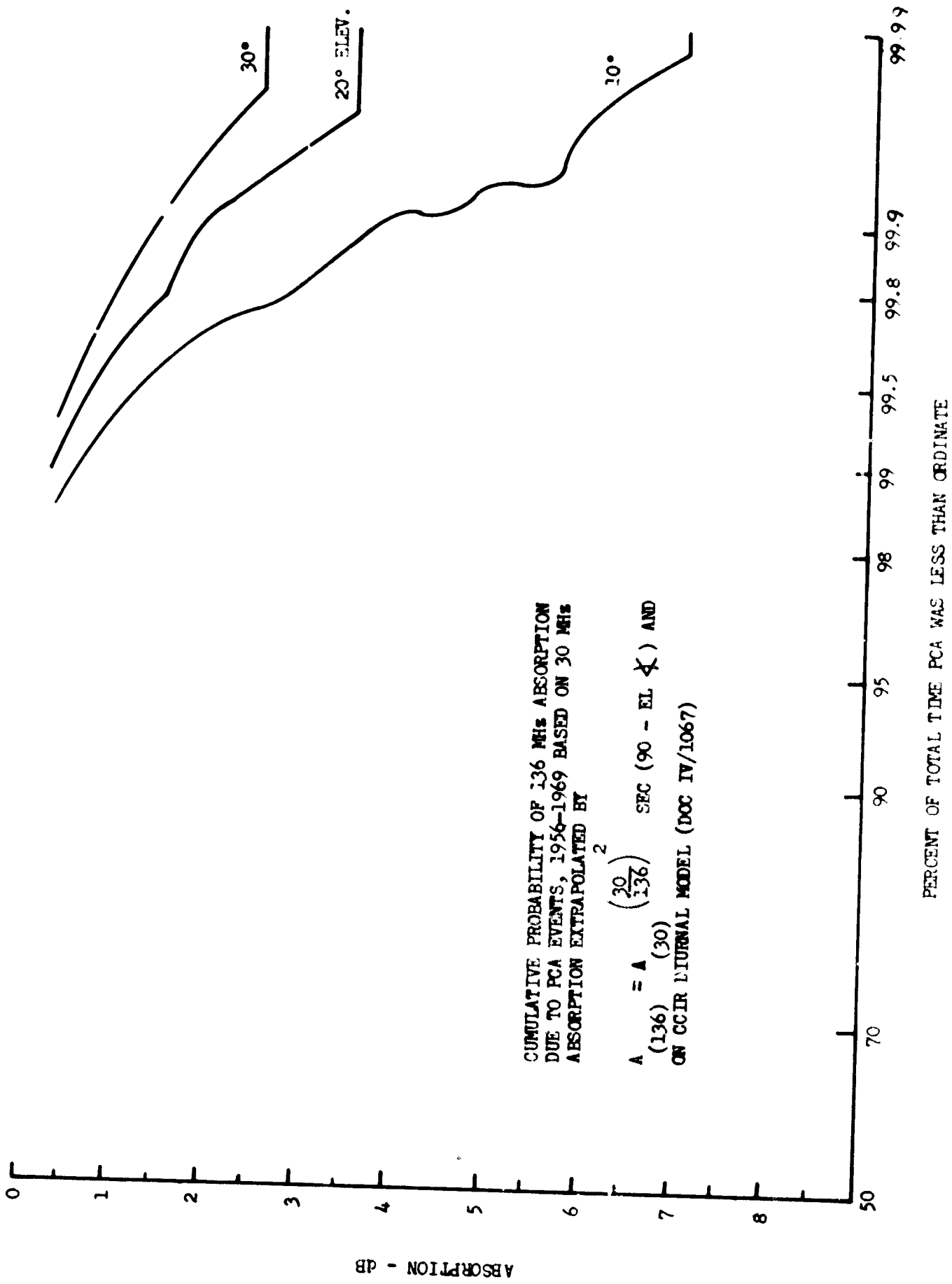
Whitney⁽²⁴⁾ computed the cumulative probability of 136 MHz absorption at 10°, 20° and 30° elevation angles employing the peak value and diurnal model previously discussed. The results of these computations are shown in Figure 11. It should be noted that in the 14 years covered by these statistics, there are approximately 10^4 half days. Thus, the tails of the curves above 99.0% and 99.9% are equivalent to 100 and 10 half days or approximately 33 and 3 events respectively. Thus it can be seen that only a very few events are responsible for the higher absorption values that might have a large effect on systems performance.

The cumulative probability distribution in Figure 11 was scaled back to 27.6 MHz vertical riometer equivalent to form a basis for the geographical contours of PCA contained in this report. These values were as follows:

| <u>Percent time PCA value</u> | <u>PCA value (db)</u> |
|-------------------------------|-----------------------|
| 95% | 0 |
| 99% | 2.0 |
| 99.9% | 13.7 |

3.3.9 Geographical Distribution of PCA in the North Atlantic

The absorption magnitude at various geographic locations was established by scaling the 27.6 MHz vertical riometer data to 136 MHz by both $1/f^2$ and $1/f^{1.4}$ frequency dependence. Also the elevation angle dependence was scaled by both the D-layer geometry assuming an homogeneous ionosphere and by the secant of the zenith angle. In order to bracket the best and worst case conditions, two



CUMULATIVE PROBABILITY OF 136 MHz ABSORPTION
 DUE TO PCA EVENTS, 1956-1969 BASED ON 30 MHz
 ABSORPTION EXTRAPOLATED BY

$$A = A \left(\frac{20}{136} \right)^2 \text{ SEC } (90 - \text{EL } \angle) \text{ AND}$$

(136) (30)
 ON CCIR DIURNAL MODEL (DOC IV/1067)

Figure 11. Polar Cap Absorption (Reproduced from Whitney, Ref. 24.)

combinations were employed: (1) $1/f^2$ was combined with the D-layer geometry to provide the best case and (2) $1/f^{1.4}$ was combined with the secant of the zenith angle to provide the worst case. It is believed that the real case should fall between these two extremes.

Assuming two locations for equatorial synchronous satellites in a North Atlantic aeronautical satellite system, it is then possible to generate contours of PCA employing the assumptions and model described above. Figures 12 through 15 show such contours for each satellite and best and worst case assumptions for frequency and elevation angle scaling. The assumptions employed in generating these contours are contained in the notes accompanying each figure. It can be seen that once the position of the satellite is determined and certain assumptions are made concerning the geographic extension of the data, the contours become fixed and one can assign a family of values depending on the time availability one desires. Thus, the four maps may be used within reasonable tolerances for other peak values and distributions by substituting in the contour tables accompanying each map a new value obtained by scaling the old value (in db) by the appropriate ratio (in db) between the new distribution and the one shown in Figure 11.

The contours in figures 12 thru 15 appear similar to those published by Pope⁽²⁶⁾ which are reproduced in figure 16. There are, however several significant differences:

- (1) The values on Pope's contours are the ratio between 137 MHz and the 30 MHz absorption well within the polar cap region. Therefore, the values must be multiplied by some assumed cumulative probability in order to compare them to the contours in this report.

- (2) Pope's contours assume a geomagnetic index (Kp) of 4 which is only moderate and does not therefore include the effects of the southward shift that would occur when magnetic storms accompany PCA events. (See paragraph 3.3.2 above)
- (3) The curves are based upon a characteristic rigidity of $P_0 = 100$ Mv and therefore do not include the effects of this variable which may typically range between 45 and 375 Mv.

Pope provides a statistical cumulative hours of absorption at various levels which may be used in conjunction with his geographical contours. These were not used in this report because they are plotted only for the years 1958, 1959 and 1960 which represent only high sunspot years and the plots were obtained by taking the envelope of the decay of the individual absorption events and therefore did not include the diurnal statistics of each event.

3.3.10 Conclusions

Evaluating the impact of PCA on a system power budget for an aeronautical satellite system presents somewhat of a dilemma. On the one hand, the rarity of the occurrence of PCA's sufficiently great as to affect the system,

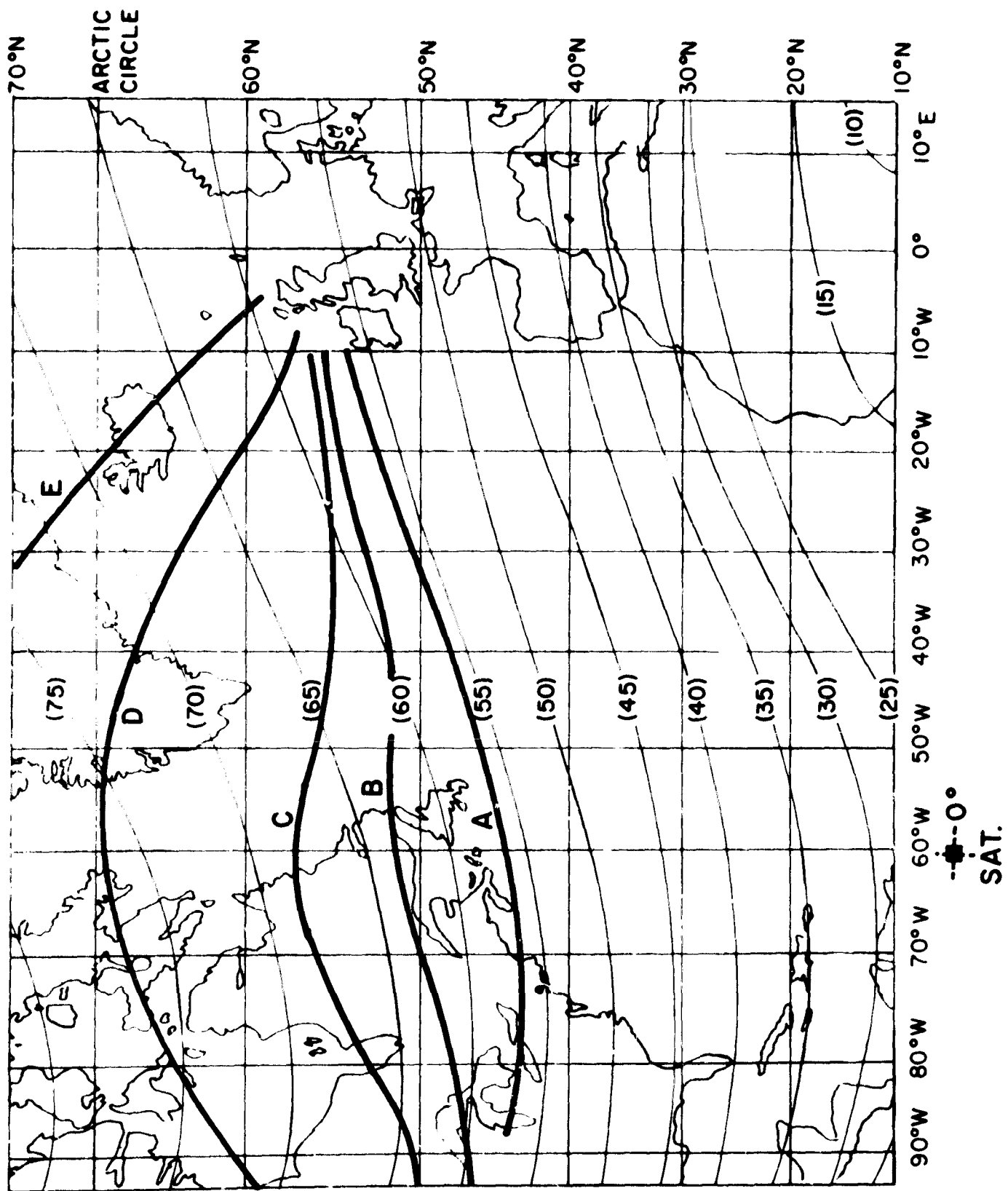


Figure 12. Contours of Polar Cap Absorption of 136 MHz Signals
 From a 60°W Equatorial Satellite (Best Case
 Geometric and Frequency Scaling)
 (See notes next page)

Figure 12. Contours of Polar Cap Absorption of 136 MHz Signals from a 60° W. Equatorial Satellite (Best case geometric and frequency scaling)

- Notes: 1. Frequency scaling: $1/f^2$
 2. Zenith angle scaling: Spherical D-layer (50 - 90 km)
 3. Absorption contour values in db:

| | <u>Contour</u> | | | | |
|-------|----------------|----------|----------|----------|----------|
| | <u>A</u> | <u>B</u> | <u>C</u> | <u>D</u> | <u>E</u> |
| 95% | 0 | 0 | 0 | 0 | 0 |
| 99.0% | 0.09 | 0.13 | 0.17 | 0.22 | 0.28 |
| 99.9% | 0.34 | 0.77 | 1.1 | 1.5 | 1.9 |

4. Data Sources

- a) Vertical riometer data at 27.6 MHz
- b) CCIR Diurnal Model (Doc. IV/1067)
- c) Events of 1956-1969 (After Whitney, Ref. 24)

5. Geographic extension assumptions:

- a) PCA is homogeneous at max value at 65° invariant latitude and above.
- b) PCA drops to 3/4 at 60° invariant latitude.
- c) PCA drops further to 1/2 at 57° invariant latitude.
- d) PCA non-existent at and below 55° invariant latitude.

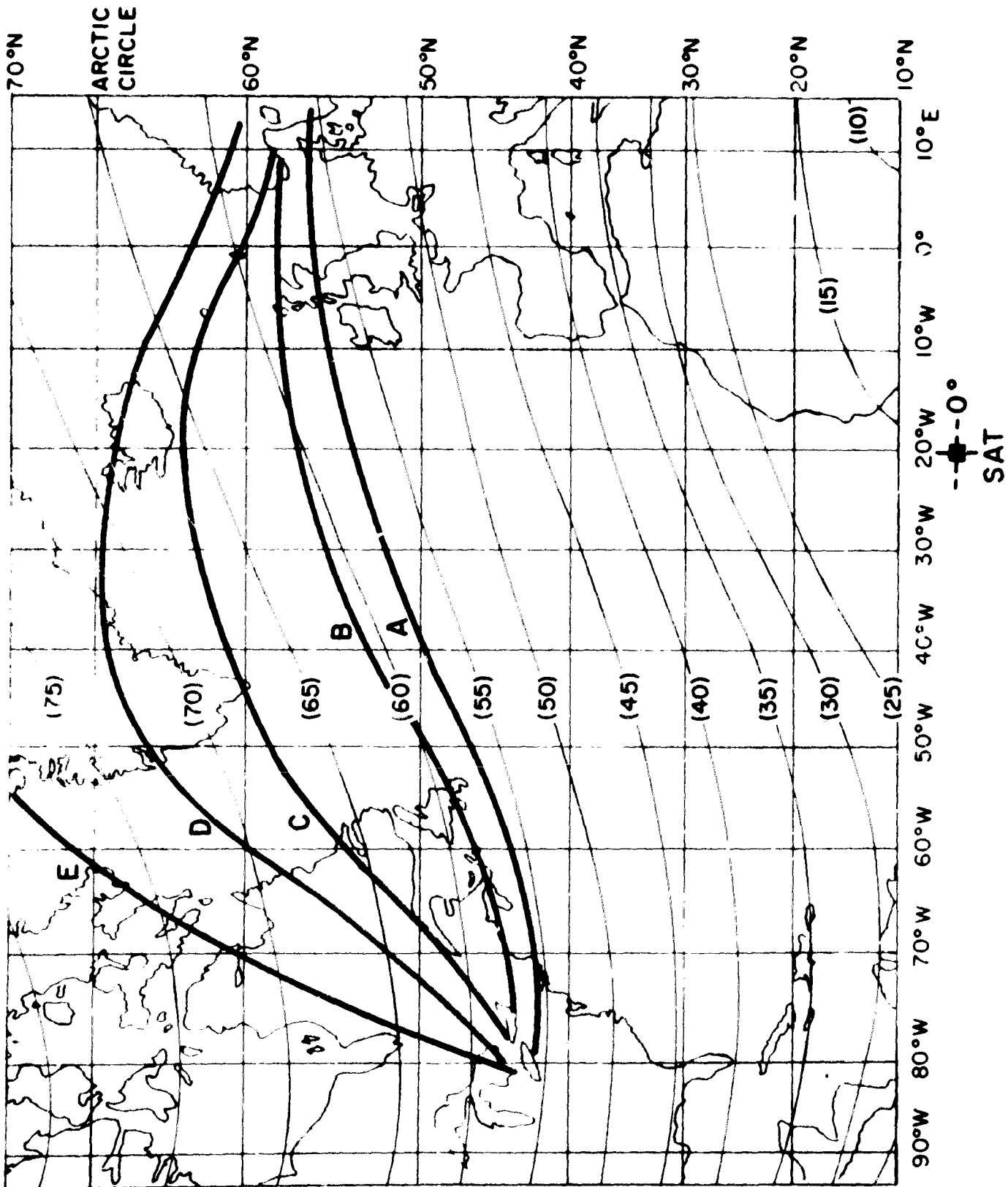


Figure 13. Contours of Polar Cap Absorption of 126 MHz Signals
 From a 200W Equatorial Satellite (Best Case
 Geometric and Frequency Scaling)
 (See notes next page)

Figure 13. Contours of Polar Cap Absorption of 136 MHz Signals from a 20° W. Equatorial Satellite (Best case geometric and frequency scaling)

- Notes: 1. Frequency scaling: $1/f^2$
2. Zenith angle scaling: Spherical D-layer (50-90 km)
3. Absorption contour values in db:

| | <u>A</u> | <u>B</u> | <u>C</u> | <u>D</u> | <u>E</u> |
|-------|----------|----------|----------|----------|----------|
| 95% | 0 | 0 | 0 | 0 | 0 |
| 99.0% | 0.09 | 0.13 | 0.17 | 0.22 | 0.28 |
| 99.9% | 0.34 | 0.77 | 1.1 | 1.5 | 1.9 |

4. Data Sources

- a) Vertical riometer data at 27.6 MHz
- b) CCIR Diurnal Model (Doc. IV/1067)
- c) Events of 1956-1969 (After Whitney, Ref. 24)

5. Geographic extension assumptions

- a) PCA is homogeneous at max. value at 65° invariant latitude and above.
- b) PCA drops to 3/4 at 60° invariant latitude.
- c) PCA drops further to 1/2 at 57° invariant latitude.
- d) PCA non-existent at and below 55° invariant latitude.

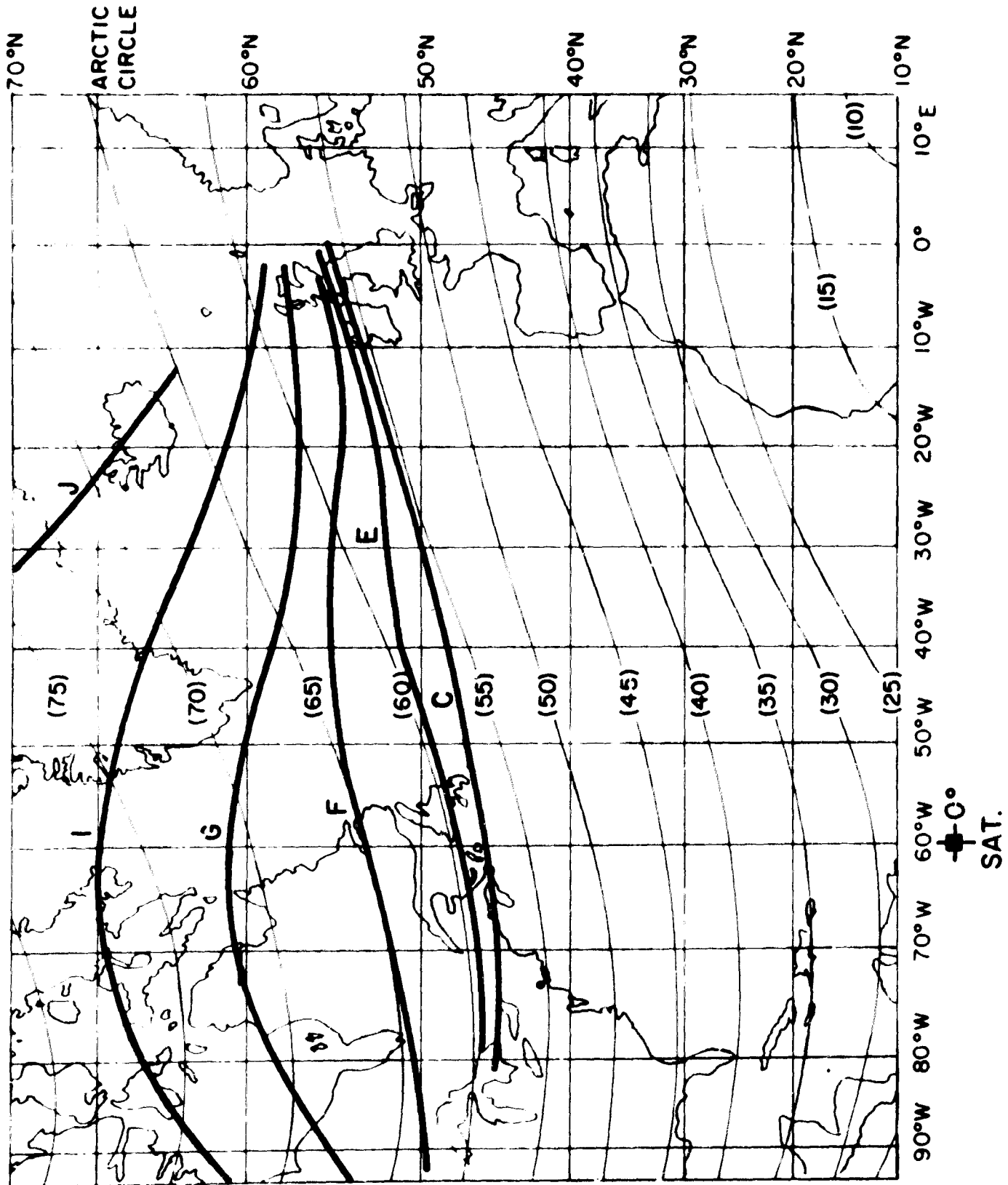


Figure 14. Contours of Polar Cap Absorption of 136MHz Signals
 From a 60°W Equatorial Satellite (Worst Case
 Geometric and Frequency Scaling)
 (See notes next page)

Figure 14. Contours of Polar Cap Absorption of 136 MHz Signals from a 60° W. Equatorial Satellite (Worst case geometric and frequency scaling)

Notes: 1. Frequency scaling: $1/f^{1.4}$

2. Zenith angle scaling: Secant

3. Absorption contour values in db:

| | <u>Contour</u> | | | | | |
|-------|----------------|----------|----------|----------|----------|----------|
| | <u>C</u> | <u>E</u> | <u>F</u> | <u>G</u> | <u>I</u> | <u>J</u> |
| 95% | 0 | 0 | 0 | 0 | 0 | 0 |
| 99.0% | 0.2 | 0.3 | 0.4 | 0.5 | 0.7 | 1.1 |
| 99.9% | 1.2 | 2.0 | 2.3 | 3.5 | 4.6 | 7.0 |

4. Data Sources

- a) Vertical riometer data at 27.6 MHz
- b) CCIR Diurnal Model (Do. IV/1067)
- c) Events of 1956-1969 (After Whitney, Ref. 24)

5. Geographic extension assumptions

- a) PCA is homogeneous at max value at 65° invariant latitude and above.
- b) PCA drops to 3/4 at 60° invariant latitude.
- c) PCA drops further to 1/2 at 57° invariant latitude.
- d) PCA non-existent at and below 55° invariant latitude.

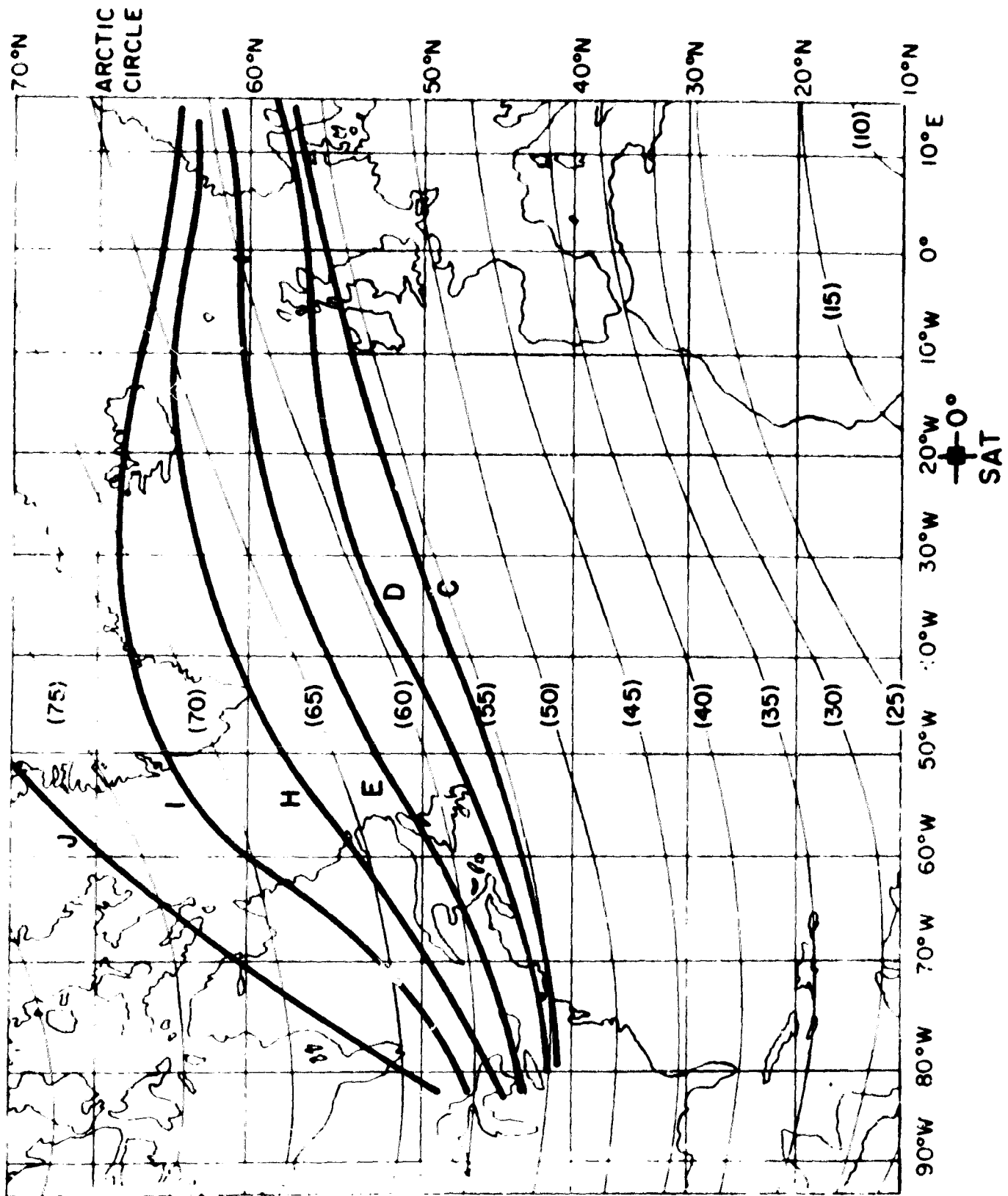


Figure 15. Contours of Polar Cap Absorption of 136MHz signals
 From a 20°W Equatorial Satellite (Worst Case
 Geometric and Frequency Scaling)
 (See notes next page)

Figure 15. Contours of Polar Cap Absorption of 136 MHz Signals from a 20° W. Equatorial Satellite. (Worst case geometric and frequency scaling.)

Notes: 1. Frequency scaling: $1/f^{1.4}$

2. Zenith angle scaling: Secant

3. Absorption contour values in db:

| | <u>Contour</u> | | | | | |
|-------|----------------|----------|----------|----------|----------|----------|
| | <u>C</u> | <u>D</u> | <u>E</u> | <u>H</u> | <u>I</u> | <u>J</u> |
| 95% | 0 | 0 | 0 | 0 | 0 | 0 |
| 99.0% | 0.2 | 0.25 | 0.3 | 0.6 | 0.7 | 1.1 |
| 99.9% | 1.2 | 1.5 | 2.0 | 3.9 | 4.6 | 7.0 |

4. Data Sources

- a) Vertical riometer data at 27.6 MHz
- b) CCIIR Diurnal Model (Do. IV/1067)
- c) Events of 1956-1969 (After Whitney, Ref. 24)

5. Geographic extension assumptions

- a) PCA is homogeneous at max value at 65° invariant latitude and above.
- b) PCA drops to 3/4 at 60° invariant latitude.
- c) PCA drops further to 1/2 at 57° invariant latitude.
- d) PCA non-existent at and below 55° invariant latitude.

might lead one to a conclusion based on statistics that over an eleven year period the time availability is so high, no additional margin is required. On the other hand, the long duration of a PCA fade (in the order of several hours) leads one to conclude that the PCA could last through the duration of a whole flight and, thus, adequate allowance should be made for this event. This second possible conclusion is further affected by the probability (or lack thereof) that a PCA fade may be accompanied by scintillation fading. This dilemma cannot be resolved by propagation factors alone. Aeronautical routing and operational procedures, system design parameters, and perhaps other factors beyond the scope of this paper must be taken into consideration.

4.0 Summary and Recommendations

In this report it was concluded that no allowance need be made for tropospheric absorption but that both auroral and polar cap (ionospheric) absorption should be considered in the design of a north Atlantic aeronautical VHF system. In the case of auroral absorption between 1 and 2 db may be experienced but this should not be additive db-wise in a power budget but rather should be combined statistically with other propagation factors such as scintillation and multipath fading. PCA is statistically small when considered over a sunspot cycle but when it does occur it may cause attenuations of up to 5 or 6 db and last continuously for several hours. Therefore, it was concluded that the decision to provide a margin allowance and the technique of doing so must involve not only the propagation aspects, but must also consider the aeronautical routing and operational procedures and aeronautical telecommunications systems design. Such considerations must include a specified time frame in which the operations must maintain a desired time availability whether this be a flight, a day, a month, a

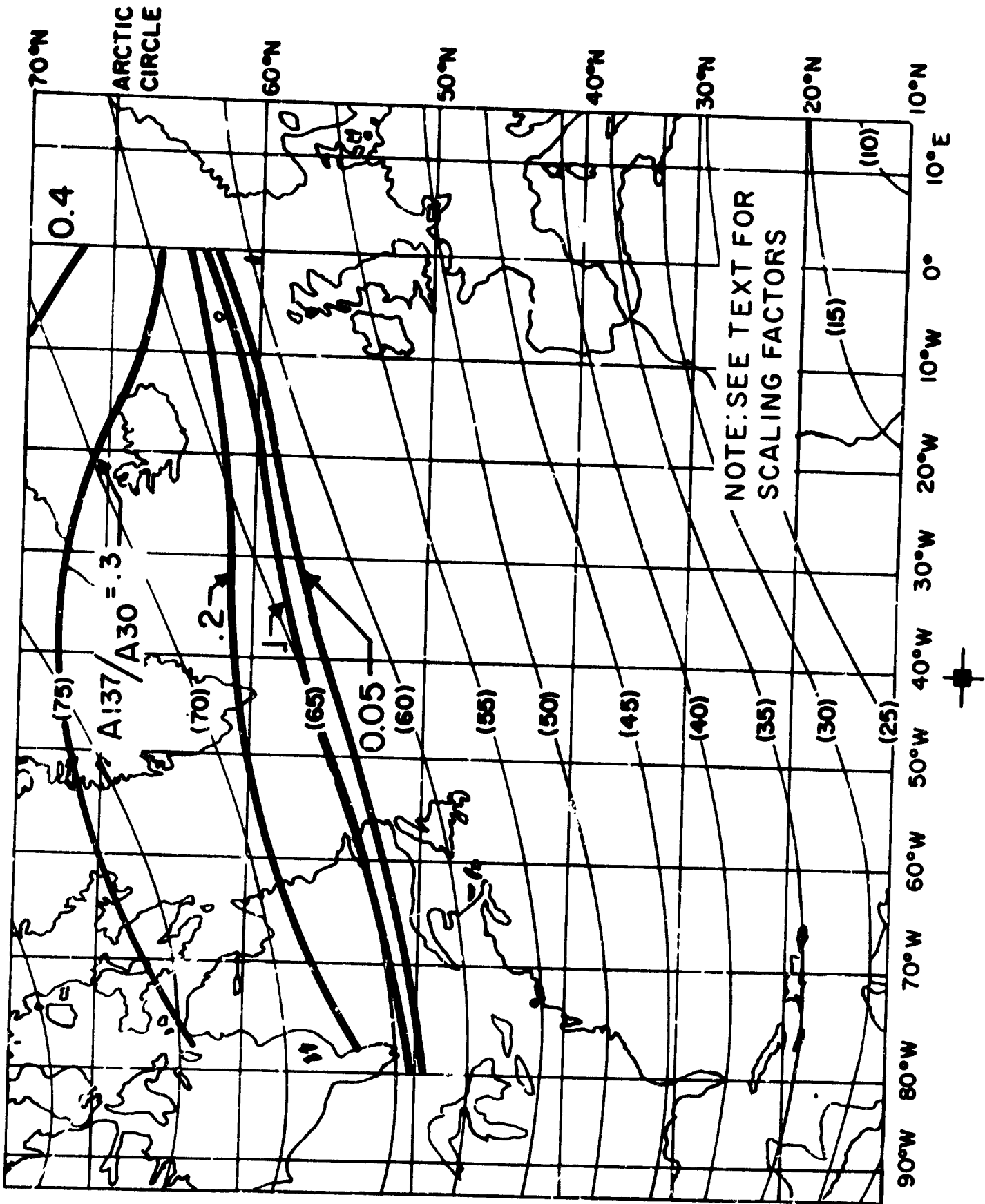


Figure 16. Contours of Oblique 137 MHz Absorption Relative to 30 MHz Polar Cap Absorption from a 40°W Equatorial Satellite. (Reproduced from Pope and Leinbach, Ref. 26)

year or a sunspot cycle. These conclusions were drawn from calculations obtained by extrapolation of data acquired by use of measuring techniques employed for studying the ionosphere and therefore are not based upon direct experience in synchronous satellite systems. The extrapolations and scaling that were necessary due to the lack of direct data have indicated that a fairly wide gap exists between the best and worst case combinations of scaling factors. Further, the data employed as a base is rather sparse and arbitrary. The frequency and elevation angle scaling of the auroral absorption data were based only on observations at one location. The PCA calculations were based on scaling of riometer data by an arbitrary diurnal model of PCA events. Perhaps the currently available information that is summarized in this paper is sufficient (when considered in the light of aeronautical routing, operational procedures and systems design) to establish a satellite power budget with sufficient accuracy to proceed with a program. However, it appears that it would be desirable to obtain more direct quantitative absorption data by measurements at high latitude stations of signals from equatorial satellites. Several stations are engaged in obtaining data on ionospheric scintillation and with perhaps very little additional effort, PCA and auroral absorption events could be identified in this data by correlation with riometer data taken simultaneously. Additionally, it would be useful to review the actual structure of previous PCA's from their riometer measurements and develop a statistical diurnal model of PCA to replace the current arbitrary one.

REFERENCES

- 1) Bean, B.R. and Dutton, E.J., Radio Meteorology, National Bureau of Standards Monograph 92, March, 1966, U.S. Govt. Printing Office.
- 2) Hargreaves, J.K., "Auroral Absorption of H.F. Radio Waves in the Ionosphere: A Review of Results from the First Decade of Riometry", Proc. IEEE, Vol. 57, No. 8, August, 1969.
- 3) Reid, G.C., "Ionospheric Disturbances", Physics of Geomagnetic Phenomena, Vol. 2, Academic Press Inc., New York, 1968.
- 4) Basler, R.P., Leinbach, H., Owren, L., "Estimated Absorption of 136 Mc/s Satellite Radio Signals", University of Alaska, NASA Contract No. NAS5-1413, Feb. 1962.
- 5) Davies, K., Ionospheric Radio Propagation, National Bureau of Standards Monograph 80, April, 1965, U.S. Govt. Printing Office.
- 6) McIlwain, C.E., "Coordinates for Mapping the Distribution of Magnetically Trapped Particles", Jour. of Geophysical Research, 66 3681, 1961.
- 7) Evans, J.E., Newkirk, L.L., McCormac, B.M., "North Polar, South Polar, World Maps and Tables of Invariant Magnetic Coordinates for Six Altitudes: 0, 100, 300, 600, 1000, and 3000 Km.", Lockheed Palo Alto Research Laboratory, Sponsored by the Defense Atomic Support Agency under NWER Subtask HCO47, October 1969.
- 8) Basler, R.P. and Owren, L., "Ionospheric Radio Wave Absorption Events and their Relation to Solar Phenomena", University of Alaska, Scientific Report under Grants GP947 and GP169, National Science Foundation, Washington, D.C., July 1964.
- 9) Lerfald, G.M., Little, C.G., and Parthasarathy, R., "D-Region Electron Density Profiles during Auroras", Journal of Geophysical Research, Vol. 69, No. 13, July 1, 1964.
- 10) Belikovich, V.V. et al, "On Frequency Dependence of Abnormal Ionospheric Absorption in the Auroral Zone", Journal of Atmospheric and Terrestrial Physics, Vol. 30, 1968.
- 11) Basler, R.P., "Radio Wave Absorption in the Auroral Ionosphere", Journal of Geophysical Research, Vol. 68, No. 16, August 15, 1963.
- 12) Hartz, T.R., Montbriand, L.E. and Vogan, E.L., "A Study of Auroral Absorption at 30 MHz", Canadian Journal of Physics, Vol. 41, (1963).
- 13) Holt, C., Landmark, B. and Lied, F., "Radiowave Absorption in the Ionosphere", (Pergamon Press, London), Chap. 21, (1962).

- 14) Hartz, T.R., "The General Pattern of Auroral Particle Precipitation and its Implications for High Latitude Communication Systems", Ionospheric Radio Communication, Plenum, New York, 1968.
- 15) Basler, R.P., "The Nature of Solar M-Regions", Planetary Space Science, Vol. 14, p 1193 (1966).
- 16) Levatich, J.L., "Absorption of 136 MHz Satellite Signals", Comsat Technical Memorandum SAD-3-67, April 17, 1967.
- 17) "Technical Characteristics of Communication Satellite Service to Aircraft and Ships", Proposed revision to Draft Report L.4.d (Document IV/430-E) U.S. C.C.I.R. Study Group IV-c, (Document approved at XIIth Plenary Assembly, New Delhi, February 1970). To be issued as Report 504.
- 18) Reid, G.C. and Leinbach, H., "Morphology and Interpretation of the Great Polar Cap Absorption Events of May and July, 1959", Journal of Atmospheric and Terrestrial Physics, Vol. 23, pp. 216-228, Proceedings of the AGARD Ionospheric Committee, Fifth Meeting, Athens, Greece.
- 19) Bailey, D.K., "Polar Cap Absorption", Planetary and Space Science, 1964, Vol. 12, pp 495 to 541.
- 20) Leinbach, H., "Midday Recoveries of Polar Cap Absorption", Journal of Geophysical Research, Vol. 72, No. 21, Nov. 1, 1967.
- 21) Leinbach, H., Venkatesan, D., and Parthasarathy, R., "The Influence of Geomagnetic Activity on Polar Cap Absorption", Planetary and Space Science, 1965, Vol. 13, pp 1075 to 1095.
- 22) Reid, G.C., Private communication.
- 23) Bennett, S.M. and Rourke, G.F., "Effects on Non-Inverse-Frequency-Squared Absorption Events", Propagation Factors in Space Communication, Chapter 3-13, AGARD Conference Proceedings No. 3, 1967, W. and J. MacKay and Co., Ltd., London and Chatham, England.
- 24) Whitney, H.E., "Estimation of Effects of Polar Cap Absorption on VHF Signals Received at High Latitude Stations", Air Force Cambridge Research Laboratories, Bedford, Mass.
- 25) Calvit, T., Communication Satellite Corp., Private Communication.
- 26) Pope, J. H. and Leinbach, H. "Effects of Polar Cap Absorption Events on Geostationary Satellite Communications Systems." National Oceanic and Atmospheric Administration, Environmental Research Laboratories, Boulder, Colo. October 1970.
- 27) Lansinger, J. M., "Auroral Zone Radio Star Scintillation Measurements and Interpretations", Propagation Factors in Space Communication, Chapter 3-12, AGARD Conference Proceedings No. 3, 1967, W. and J. MacKay and Co. Ltd., London and Chatham, England.